Available online at www.sciencedirect.com

SCIENCE DIRECT®

Coordination Chemistry Reviews 246 (2003) 185–202

COORDINATION CHEMISTRY REVIEWS

www.elsevier.com/locate/ccr

Silver(I)–hexamethylenetetramine molecular architectures: from self-assembly to designed assembly

Shao-Liang Zheng, Ming-Liang Tong, Xiao-Ming Chen*

School of Chemistry and Chemical Engineering, Sun Yat-Sen University, Guangzhou 510275, China

Received 29 August 2002; accepted 19 June 2003

Contents

Abstract

The investigations on the construction of silver(I)–hexamethylenetetramine coordination networks containing different additional ligands and counter anions have been reviewed. The interesting topologies, synthetic approaches and the important factors that influence the structures, as well as some designed assembly approaches are described.

Keywords: Silver(I); Hexamethylenetetramine; Coordination polymer; Topology; Crystal engineering

1. Introduction

The construction of solid-state molecular architectures and crystal engineering have become rapidly developing research areas which have implications for the rational design of functional metal–organic materials [1–5]. Many investigations have been centered upon the use of supramolecular contacts, such as hydrogen bonding, π–π interaction between suitable molecules to generate multi-dimensional arrays or networks. In particular, these arrays or networks may exhibit potential applications in reversible guest exchange, selective catalysis, microelectronic devices, molecular magnets and so on [3–5].

It is obvious that ligation of organic bridging ligands (such as linear two-connectors, trigonal three-connectors, and tetrahedral or square-planar four-connectors) to metallic centers may give rise to organometallic frameworks with intriguing and diverse topological types. Among these networks, it is also possible that polydentate ligands assembled with linear metal centers (such as biconnected Ag(I) ions) can entirely dictate the topology of the array [6]. Hexamethylenetetramine (designated hereafter as hmt) is a

---

* Corresponding author. Tel.: +86-20-8411-3986; fax: +86-20-8411-2245.
E-mail address: cescxm@zsu.edu.cn (X.-M. Chen).

0010-8545/$ – see front matter © 2003 Elsevier B.V. All rights reserved.
doi:10.1016/S0010-8545(03)00116-4

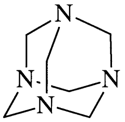

Scheme 1. Schematic representation of the structure of hmt.

well-known, simple organic compound, its crystal structure has been known for eight decades [7] (Scheme 1). As a very good hydrogen acceptor, hmt forms a variety of molecular adducts with hydrogen-donor groups via hydrogen bonding with organic molecules [8,9]. On the other hand, as a simple and potential tetradentate ligand, it exhibits different coordination modes including the monodentate and μ_n-bridging ($n = 2$–4) modes in ligating metal ions, hence generating a large amount of metal–hmt complexes. Among a large number of non-silver(I) metal complexes documented in the past several decades, they exhibit a variety of monomeric and polymeric structures [10,11].

Although the first crystal structure of Ag–hmt species was documented two decades ago [12], prior to 1995 only sporadic reports appeared in the literature. A large number of Ag–hmt compounds containing different anionic ligands or counter-anions have been reported in recent years [14–29]. This fact can be attributed to the rapid increase of interest in crystal engineering of coordination polymers in the past decade. In fact, silver(I) is very flexible in coordination to organic ligands, which usually exhibit two- to four- coordination featuring linear, T-shape and trigonal, as well as tetrahedral geometries. Therefore, it can be expected that the combination of silver(I) and hmt as building blocks can produce interesting molecular architectures, parallel to the supramolecular organic chemistry of adamantane templates with different synthons [30]. The self-assembly of silver(I) ions with hmt in different conditions, such as different Ag/hmt molar ratios, different counter anions, or different additional anionic organic ligands, may lead to different molecular architectures, as we and others have pointed out previously [31]. The so-called controlled or designed assembly can also be achieved in some cases [22,23]. This article accounts exclusively the research on crystal engineering of Ag–hmt system and outlines the network topologies and structural motifs reported so far. The synthetic approaches and the important factors that influence the structures, as well as the designed assembly approaches are described.

2. Structural motifs

Since 1995, investigations on Ag–hmt coordination polymers have significantly intensified, and much attention has been devoted to the construction of interesting supramolecular architectures. Considering exclusively the Ag–hmt interactions, a variety of structural motifs have been observed for these molecular architectures, including a discrete $[Ag_5(hmt)_6]^{5+}$ cage [17] and two zero-dimensional $[hmt \cdot 4Ag(I)]$ structural units [13,27], a one-dimensional ribbon [18], several single- and double-chains [22,27], several two-dimensional infinite undulating layers of different structural units [12,16,19–21,23,24,26–28], and different examples of three-dimensional networks, all non-interpenetrated [14–18,20,25,29], as summarized in the Table 1. It is obvious that in the Ag–hmt complexes, each hmt acts in a bridging coordination mode, such as μ_2-, μ_3-, or μ_4-bridging modes, no monodentate mode has been observed in the entire Ag–hmt system, in contrast to those found in other metal complexes of hmt [10]. Therefore, it usually plays a role as a spacer in one-dimensional chains or as a node in the two- and three-dimensional nets. Usually, hmt functions in a single bridging mode in an Ag–hmt compound, but occasionally it acts in more than one bridging mode, i.e. a mixed-bridging mode. Such mixed-bridging modes have so far been documented in $[Ag_2(\mu_2\text{-hmt})(\mu_3\text{-hmt})(H_2O)(SbF_6)]$ (**4**) [18] and $[Ag_2(\mu_2\text{-hmt})(\mu_3\text{-hmt})(ssa)]$ (ssa = sulfosalicylate) (**29**) [24] and $[Ag_8(\mu_3\text{-hmt})_2(\mu_4\text{-hmt})_2(\mu_2\text{-pma})_2(\mu_2\text{-}H_2O)_3] \cdot 18H_2O$ (pma = 1,2,4,5-benzenetetracarboxylate) (**42**) [29]. On the other hand, the usual coordination number of Ag(I) is 2–4, spanning the linear, T-shaped (or Y-shaped) and tetrahedral geometries. An exceptional distorted octahedral coordination of Ag(I) has been documented recently in $[Ag_2(\mu_4\text{-hmt})(\mu_4\text{-ox})]$ (ox = oxalate) (**23**) [20b].

2.1. Zero-dimensional motifs

Considering only the Ag–hmt interactions, the $[Ag_4(hmt)]^{4+}$ core structure of $[Ag_4(\mu_4\text{-hmt})X_4]$ ($X = Cl^-$, Br^-) (**1**) may be regarded as zero-dimensional (Fig. 1a), however, they are in fact extended to a three-dimensional framework by the μ_3-Cl^- or μ_3-Br^- bridges (Fig. 1b) [13]. Analogous $[Ag_4(\mu_4\text{-hmt})]^{4+}$ core structures have also been found in $[Ag_4(\mu_4\text{-hmt})(\mu_4\text{-}\eta^2\text{-nda})_2] \cdot 2H_2O$ (nda = 2,6-naphthalenedicarboxylate) (**2**), which are bridged into a three-dimensional network by the carboxylate groups [27]. Thus, $[Ag_5(\mu_2\text{-hmt})_6](PF_6) \cdot 3CH_2Cl_2$ (**3**) is an unique example showing a zero-dimensional motif, which consists of a large, pentanuclear $[Ag_5(\mu_4\text{-hmt})_6]^{5+}$ cation possessing an idealized D_{3h} symmetry, as illustrated in Fig. 2 [17]. The six hmt ligands are biconnected and are disposed at the corners of a trigonal prism. Two of the Ag(I) atoms are triconnected and placed at the centers of the two triangular faces, while the other three metal atoms bridge the lateral edges. The three PF_6^- anions are weakly coordinated to the Ag(2) atoms.

In other words, since both silver(I) and hmt species can act in bridging modes, their complexes are usually polymeric, and only a few very unusual cases exhibit discrete structures if only the Ag–hmt interactions are taken into consideration.

2.2. One-dimensional motifs

Taking only the Ag–hmt interactions into consideration, there are three types of one-dimensional structural mo-

Table 1
The structurally characterized Ag(I)–hmt polymeric species

Number	Compound		Network [a]	Reference
1	$[Ag_4(\mu_4\text{-hmt})X_4]$ (X = Cl^-, Br^-)	0-D		[13]
2	$[Ag_4(\mu_4\text{-hmt})(\mu_4\text{-}\eta^2\text{-nda})_2]\cdot 2H_2O$	0-D		[27]
3	$[Ag_5(\mu_2\text{-hmt})_6](PF_6)\cdot 3CH_2Cl_2$	0-D	D_{3h} cage	[17]
4	$[Ag_2(\mu_2\text{-hmt})(\mu_3\text{-hmt})(H_2O)(SbF_6)]$	1-D	Ribbons	[18]
5	$[Ag_2(\mu_2\text{-hmt})_2(\mu_2\text{-bi-}\eta^2\text{-bna})]\cdot 2H_2O\cdot MeCN$	1-D	Chains	[27]
6	$[Ag(\mu_2\text{-hmt})(L)(H_2O)]$ (L = hba, aba)	1-D	Chains	[22]
7	$[Ag_2(\mu_2\text{-hmt})_2(bca)(H_2O)_2]\cdot H_2O$	1-D	Chains	[22]
8	$[Ag(\mu_2\text{-hmt})(ina)]\cdot 0.5H_2O$	1-D	Chains	[22]
9	$[Ag(\mu_2\text{-hmt})(bsa)]$	1-D	Double-chains	[22]
10	$[Ag_2(\mu_2\text{-hmt})_2(bda)]\cdot 4H_2O$	1-D	Double-chains	[22]
11	$[Ag(\mu_3\text{-hmt})](ClO_4)$	2-D	Hexagons	[16]
12	$[Ag_2(\mu_3\text{-hmt})_2](S_2O_6)\cdot 2H_2O$	2-D	Hexagons	[20]
13	$[Ag(\mu_3\text{-hmt})(L)]$ (L = NO_3^-, NO_2^-)	2-D	Hexagons	[12,20]
14	$[Ag_2(\mu_3\text{-hmt})_2(CF_3SO_3)(H_2O)](CF_3SO_3)\cdot H_2O$	2-D	Hexagons	[21]
15	$[Ag(\mu_3\text{-hmt})(L)]\cdot nH_2O$ (L = *p*-nba, *m*-nba, dnba)	2-D	Hexagons	[23]
16	$[Ag_2(\mu_3\text{-hmt})_2(L)]\cdot nH_2O$ (L = fa, adp, ppa)	2-D	Hexagons	[19,23]
17	$[Ag(\mu_3\text{-hmt})(L)]\cdot nH_2O\cdot mEtOH$ (L = α-hna, β-hna, noa)	2-D	Hexagons	[23]
18	$[Ag(\mu_3\text{-hmt})(L)]\cdot nH_2O$ (L = ma, ba, sal)	2-D	Hexagons	[26]
19	$[Ag_2(\mu_3\text{-hmt})_2(MeCN)](ClO_4)_2$	2-D	Hexagons	[26]
20	$[Ag(\mu_3\text{-hmt})](L)\cdot n(\text{benzene})\cdot mH_2O$ (L = abs, ns)	2-D	Hexagons	[28]
21	$[Ag(\mu_3\text{-hmt})]_2[Ag(NH_3)_2]_2(pma)\cdot 3H_2O$	2-D	Hexagons	[28]
22	$[Ag_2(\mu_4\text{-hmt})(L)_m]\cdot nH_2O$ (L = NO_2^-, SO_4^{2-})	2-D	Squares	[20]
23	$[Ag_2(\mu_4\text{-hmt})(\mu_4\text{-ox})]$	2-D	Squares	[20]
24	$[Ag_2(\mu_4\text{-hmt})(tos)_2]$	2-D	Squares	[21]
25	$[Ag_2(\mu_4\text{-hmt})(\eta^2\text{-}\alpha\text{-hna})(MeCN)](\alpha\text{-hna})\cdot H_2O$	2-D	Squares	[27]
26	$[Ag_3(\mu_3\text{-hmt})_2(H_2O)_4](PF_6)_3$	2-D	Big hexagons	[21]
27	$[Ag(\mu_2\text{-hmt})(cin)]\cdot 2H_2O$	2-D	Compressed hexagons	[24]
28	$[Ag_2(\mu_3\text{-hmt})(sal)_2]$	2-D	Decagons and small hexagons	[24]
29	$[Ag_2(\mu_2\text{-hmt})(\mu_3\text{-hmt})(ssa)]$	2-D	Decagons	[24]
30	$[Ag_4(\mu_3\text{-hmt})_3(H_2O)](PF_6)_4\cdot 3EtOH$	3-D	3-C	[17]
31	$[Ag(\mu_3\text{-hmt})](PF_6)\cdot H_2O$	3-D	3-C	[14]
32	$[Ag_{12}(\mu_4\text{-hmt})_6(HPO_4)(H_2PO_4)_{10}(H_2O)](H_3PO_4)\cdot 10.5H_2O$	3-D	4-C	[20]
33	$[Ag_2(\mu_4\text{-hmt})(NO_3)_2]$	3-D	4-C	[15]
34	$[Ag_3(\mu_4\text{-hmt})_2(H_2O)_2](ClO_4)_3$	3-D	3,4-C	[20]
35	$[Ag_3(\mu_4\text{-hmt})_2(H_2O)_2](SO_4)(HSO_4)\cdot 2H_2O$	3-D	3,4-C	[20]
36	$[Ag_3(\mu_4\text{-hmt})_2(\mu_2\text{-ssa})(H_2O)](NO_3)\cdot 3H_2O$	3-D	3,4-C	[29]
37	$[Ag_{11}(\mu_4\text{-hmt})_6(H_2O)_{10}](PF_6)_{11}\cdot 4H_2O$	3-D	3,4-C	[18]
38	$[Ag_4(\mu_4\text{-hmt})_3(H_2O)](SO_4)(NO_3)_2\cdot 3H_2O$	3-D	3,4-C	[20]
39	$[Ag_2(\mu_4\text{-hmt})(\mu_2\text{-}O_2CMe)](MeCO_2)\cdot 4.5H_2O$	3-D	3,4-C	[20]
40	$[Ag_2(\mu_4\text{-hmt})(\mu_3\text{-L})]\cdot nH_2O$ (L = mal, oga, mpa)	3-D	3,4-C	[20,25]
41	$[Ag_3(\mu_4\text{-hmt})(\mu_2\text{-ba})_3]$	3-D	3,4-C	[20]
42	$[Ag_8(\mu_3\text{-hmt})_2(\mu_4\text{-hmt})_2(\mu_2\text{-pma})_2(\mu_2\text{-}H_2O)_3]\cdot 18H_2O$	3-D	3,4-C	[29]

Abbreviations: aba, 4-aminobenzoate; abs, 4-aminobenzenesulfonate; adp, adipate; ba, benzoate; bca, 4,4′-biphenyldicarboxylate; bda, butanedioate; bna, 2,2′-dihydroxy-1,1′-binaphthalene-3,3′-dicarboxylate; bsa, benzenesulfinate; cin, cinnamate; dnba, 3,5-di-nitrobenzoate; fa, fumarate; hba, 4-hydroxybenzoate; hmt, hexamethylenetetramine; α-hna, 1-hydroxy-2-naphthate; β-hna, 3-hydroxy-2-naphthate; ina, isonicotinate; ma, malonate; mal, maleate; mpa, *m*-phthalate; *m*-nba, 3-nitrobenzoate; *p*-nba, 4-nitrobenzoate; nda, 2,6-naphthalenedicarboxylate; noa, 2-naphthoxyacetate; ns, 2-naphthalene-sulfonate; oga, diglycolate; ox, oxalate; ppa, *p*-phthalate; pma, 1,2,4,5-benzenetetracarboxylate; sal, salicylate; ssa, sulfosalicylate; tos, *p*-toluenesulfonate.

[a] Only the Ag–hmt interactions are considered.

tifs hitherto documented in the literature, namely ribbons, single- and double-chains.

As shown as Fig. 3 $[Ag_2(\mu_2\text{-hmt})(\mu_3\text{-hmt})(H_2O)(SbF_6)]$ (**4**) features a new one-dimensional ribbon [18], in which two different types of Ag(I) atoms are located at the central and external parts of the ribbon, respectively, while hmt molecules act in an unprecedented mixed μ_2-/μ_3-bridging mode. In the Ag–hmt interactions, the internal Ag(I) atoms and hmt are triconnected, while the external ones are bi-connected. However, each Ag(I) atom interacts with an aqua ligand, and the external ones show an additional Ag–F(SbF_5) contact.

Regarding the Ag–hmt interactions, four complexes, $[Ag_2(\mu_2\text{-hmt})_2(\mu_2\text{-bi-}\eta^2\text{-bna})]\cdot 2H_2O\cdot MeCN$ (bna = 2,2′-dihydroxy-1,1′-binaphthalene-3,3′-dicarboxylate) (**5**), $[Ag(\mu_2\text{-hmt})(L)(H_2O)]$ (L = 4-hydroxybenzoate or 4-aminobenzoate) (**6**), $[Ag_2(\mu_2\text{-hmt})_2(bca)(H_2O)_2]\cdot H_2O$ (bca = 4,4′-biphenyldicarboxylate) (**7**), and $[Ag(\mu_2\text{-hmt})(ina)]\cdot 0.5H_2O$ (ina = isonicotinate) (**8**) all consist of the infinite zigzag $[Ag(\mu_2\text{-hmt})]_\infty$ chains (Fig. 4a); while $[Ag(\mu_2\text{-hmt})(bsa)]$

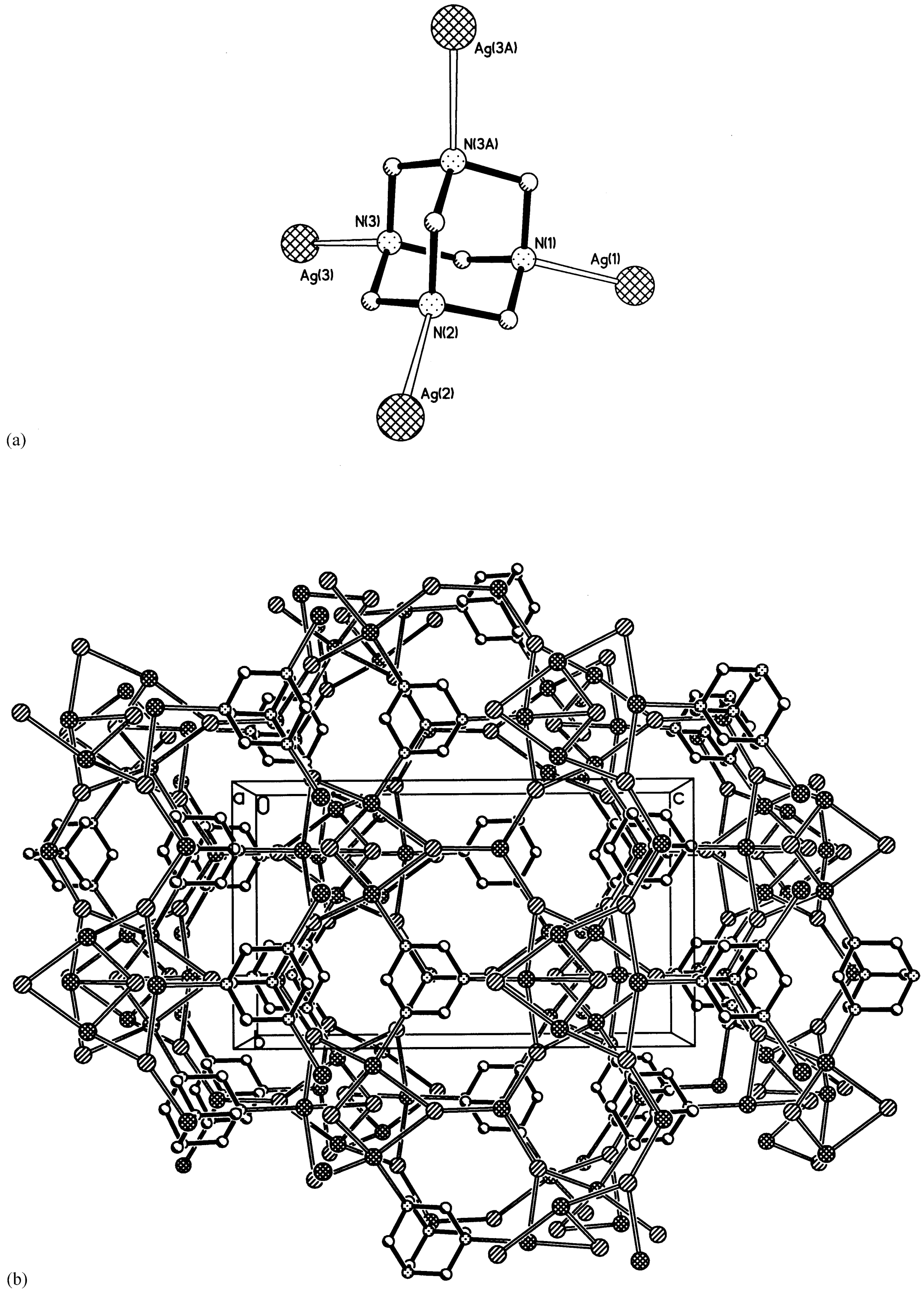

Fig. 1. The [hmt · 4Ag(I)] structural unit (a) and the three-dimensional network viewed along the *a*-axis (b) in **1** (adapted from Ref. [13]).

(bsa = benzenesulfinate) (**9**) and $[Ag_2(\mu_2\text{-hmt})_2(bda)] \cdot 4H_2O$ (bda = butanedioate) (**10**) consist of double-chains which are made up of a pair of $[Ag(\mu_2\text{-hmt})]_\infty$ chains, featuring the dimeric Ag(I) fragments with the Ag···Ag distance of 2.9–3.0 Å, indicating a relatively strong Ag···Ag interaction (Fig. 4b) [32]. Both Ag(I) and hmt usually act in the μ_2-bridging modes in the Ag–hmt interconnections among the one-dimensional chains, and additional oxygen donor ligands, such as carboxylate groups are present. These additional ligands may play a role in terminating further

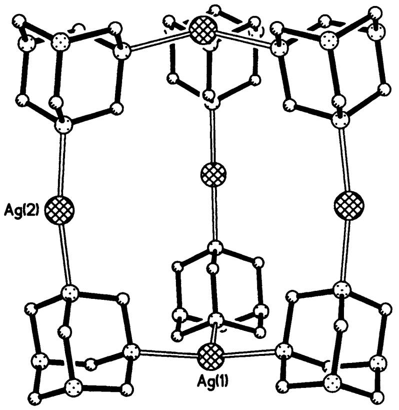

Fig. 2. Perspective view of pentanuclear [$Ag_5(hmt)_6]^{5+}$ cage in **2** (adapted from Ref. [17]).

polymerization of the one-dimensional chains into higher dimensional structures. Moreover, the Ag–hmt molar ratio is exclusively 1:1 in the hitherto documented one-dimensional Ag–hmt complexes (see Table 1).

Some interesting related frameworks based on [Ag (μ_2-hmt)]$_\infty$ chains have been successfully synthesized by judicious choice of different anionic ligands, which will be discussed in the following paragraphs.

In the earlier reported Ag–hmt complexes, the hmt ligands are usually in the μ_3- or μ_4-bridged mode [12–21], and no complex consisting of [Ag(μ_2-hmt)]$_\infty$ chains had been documented. However, the utilization of Ag_2O, appropriate carboxylic acids and hmt, followed by dropwise addition of aqueous NH_3 solution, produced a complex system, which may be propitious to construct frameworks based on the [Ag(μ_2-hmt)]$_\infty$ chains [22]. Moreover, the dimeric Ag(I) fragments can be joined by two unusual non-coplanar skew–skew μ_2-carboxylate bridges [20,24], resulting in double-chains made up with a pair of [Ag(μ_2-hmt)]$_\infty$ chains. Consequently, by judicious choice of different anionic ligands, a series of complexes containing [Ag(μ_2-hmt)]$_\infty$ chains have been synthesized, which exhibit different, but related structures.

The Ag–hmt interactions in **6**, **7** and **8** are based on the infinite zigzag [Ag(μ_2-hmt)]$_\infty$ chains, while **9** and **10** are based on [Ag(μ_2-hmt)] double-chains [22], in which all hmt ligands feature the μ_2-bridging mode. If the additional anionic ligands are taken into consideration, the coordination networks can be regarded as racks in **6**, and ladders in **7**, grids in **8**, double-chains in **9** and rectangular-grids with double-chains in **10**, as illustrated in Scheme 2. Comparing the structures, the ladder in **7** may be regarded as an extension of the single chains in **6** by replacement of the

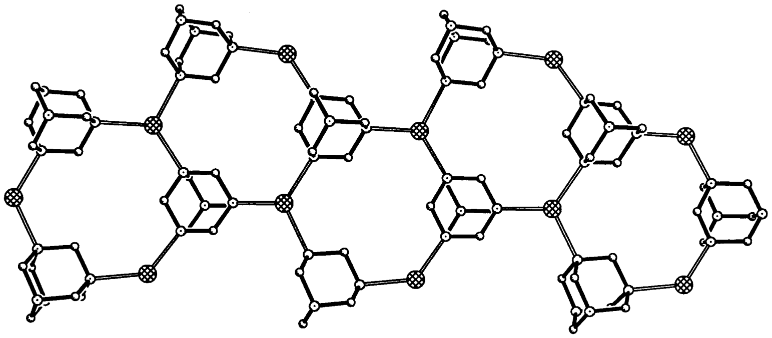

Fig. 3. Perspective view of the one-dimensional ribbon in **4** (adapted from Ref. [18]).

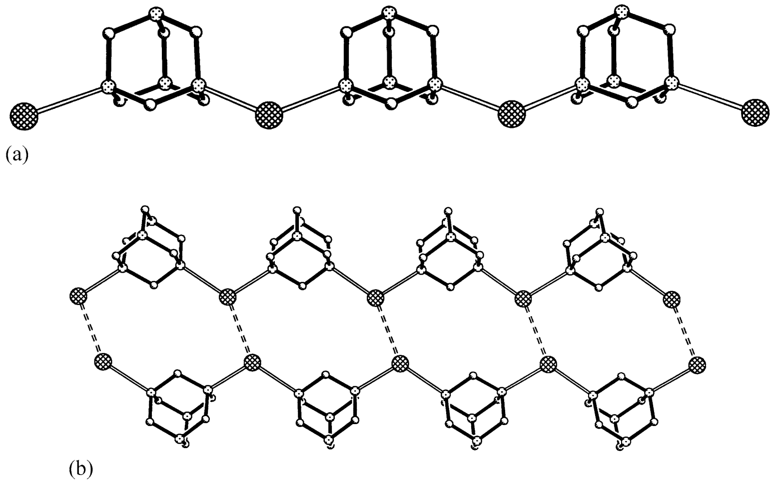

Fig. 4. Perspective views of the one-dimensional single-chain (a) and double-chain (b) (adapted from Ref. [22]).

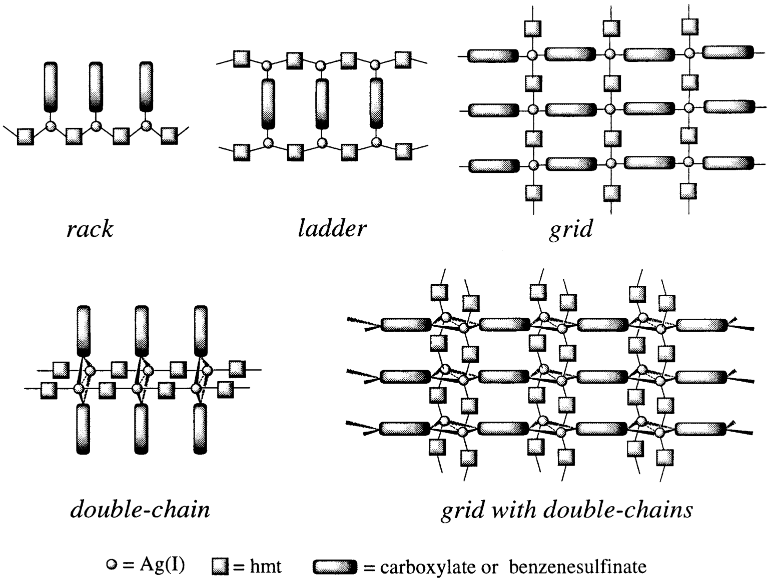

Scheme 2. The structural motifs of the coordination polymers **6**–**10** containing $[Ag(\mu_2\text{-hmt})]_\infty$ chains: racks in **6**, and ladders in **7**, grids in **8**, double-chains in **9** and rectangular-grids with double-chains in **10** (adapted from Ref. [22]).

chelate monocarboxylate ligands with the bis-monodentate dicarboxylate ligands, while the rectangular-grid layers in **8** may be regarded as an extension of the single chains in **6** by replacement of the chelate monocarboxylate ligands with the μ_2-O,N-bridging ina (ina = isonicotinate) ligands. Similarly, the rectangular-grid with double-chains in **10** may be regarded as an extension of the double-chains in **9** by replacement of the monosulfinate ligands with the dicarboxylate ligands.

2.3. Two-dimensional nets

Six types of two-dimensional Ag–hmt layers have been so far reported. Among these two-dimensional Ag–hmt layers, most consist of the hexagonal $[Ag(\mu_3\text{-hmt})]$ nets, including the first structurally characterized Ag–hmt network found in $[Ag(\mu_3\text{-hmt})(NO_3)]$ (**13**) [12].

Complexes $[Ag(\mu_3\text{-hmt})](ClO_4)$ (**11**), $[Ag_2(\mu_3\text{-hmt})_2](S_2O_6)\cdot 2H_2O$ (**12**), $[Ag(\mu_3\text{-hmt})(L)]$ ($L = NO_3^-$, NO_2^-) (**13**) and $[Ag_2(\mu_3\text{-hmt})_2(CF_3SO_3)(H_2O)](CF_3SO_3)\cdot H_2O$ (**14**) all consist of two-dimensional infinite undulating layers of hexagonal units (Fig. 5 a) [10,16,20b,21]. Each hexagonal unit is organized by three Ag(I) atoms and three hmt ligands each at the corner. Considering only the Ag–hmt interactions, the Ag(I) atoms and hmt ligands are triconnected. However, each Ag(I) atom may be further ligated by a weak bonding ligand at the lateral position of the layer, such as NO_3^- (Fig. 6) and NO_2^- anions in **13** [12,20b]. These labile lateral ligands may be replaced by other stronger ligands to produce three-dimensional molecular architectures via rational molecular design, which will be described in Section 2.5.

On the other hand, hmt can exhibit μ_4-bridging mode to connect Ag(I) atoms into two-dimensional infinite layers of square units, as found in $[Ag_2(\mu_4\text{-hmt})(L)_m]\cdot nH_2O$ ($L = NO_2^-$ or SO_4^{2-}, $m = 2$ or 1, respectively) (**22**). Each of the squares is made up of four Ag(I) atoms and four hmt ligands each at the midpoint of side and corner, respectively (Fig. 5b) [20]. When oxalate was used instead of NO_2^- or SO_4^{2-}, a new compound $[Ag_2(\mu_4\text{-hmt})(\mu_4\text{-ox})]$ (**23**) was isolated [20b], in which each square cavity is now occupied by an ox^{2-} group. The ox^{2-} group not only functions in a double chelate mode to bind two Ag(I) atoms in a pair of opposite edges of a square, but also ligates two adjacent square layers, furnishing the final three-dimensional architecture, as shown in Fig. 7.

As shown in Fig. 5c–f, there are four other topological types of two-dimensional Ag–hmt nets. Among them, $[Ag_3(\mu_3\text{-hmt})_2(H_2O)_4](PF_6)_3$ (**26**) is an undulating coordination layer with big hexagonal units, each consisting of six Ag(I) atoms and six μ_3-hmt ligands [21] (Fig. 5c); $[Ag(\mu_2\text{-hmt})(cin)]\cdot 2H_2O$ (cin = cinnamate) (**27**) is two-dimensional infinite coordination layers featuring compressed hexagonal units, each consisting of six Ag(I) atoms and four μ_2-hmt ligands as spacers (Fig. 5d); $[Ag_2(\mu_3\text{-hmt})(sal)_2]$ (sal = salicylate) (**28**) is two-dimensional infinite undulating coordination layers with decagonal and small hexagonal units, each decagonal unit composes of six Ag(I) atoms and four μ_3-hmt ligands, and each small hexagonal unit composes of four Ag(I) atoms and two μ_3-hmt ligands (Fig. 5e); while $[Ag_2(\mu_2\text{-hmt})(\mu_3\text{-hmt})(ssa)]$ (**29**) is two-dimensional infinite highly undulated neutral layers with irregular decagonal units, each consisting of five Ag(I) atoms and five hmt ligands, of which three are in a μ_3-bridging mode and two are in a μ_2-bridging mode (Fig. 5f) [24]. It should be pointed out that both **27** and **28** are constructed by dimeric Ag(I) fragments in the two-dimensional Ag–hmt nets.

It is noteworthy that, from the topological point of view, the two-dimensional motifs in Fig. 5a, c, d, f can be rationalized as the same topology, a three-connected net with (6,3) topology, comprised of six connected nodes shared by seven hexagons or seven decagons. On the other hand, the motif of Fig. 5b can be rationalized as a four-connected net with a (4,4) topology; while that of Fig. 5e is a net with (4.8^2) topology, which was predicted by Wells and has also been documented in sporadic reports recently [33].

2.4. Three-dimensional frameworks

The self-assembly of the potential tetradentate ligand hmt with the coordinative flexible Ag(I) atoms can produce interesting molecular architectures. Thus a variety of three-dimensional networks, all non-interpenetrated, have been observed.

The structure of $[Ag_4(\mu_3\text{-hmt})_3(H_2O)](PF_6)_4 \cdot 3EtOH$ (**30**) exhibits common geometric motifs in a unique struc-

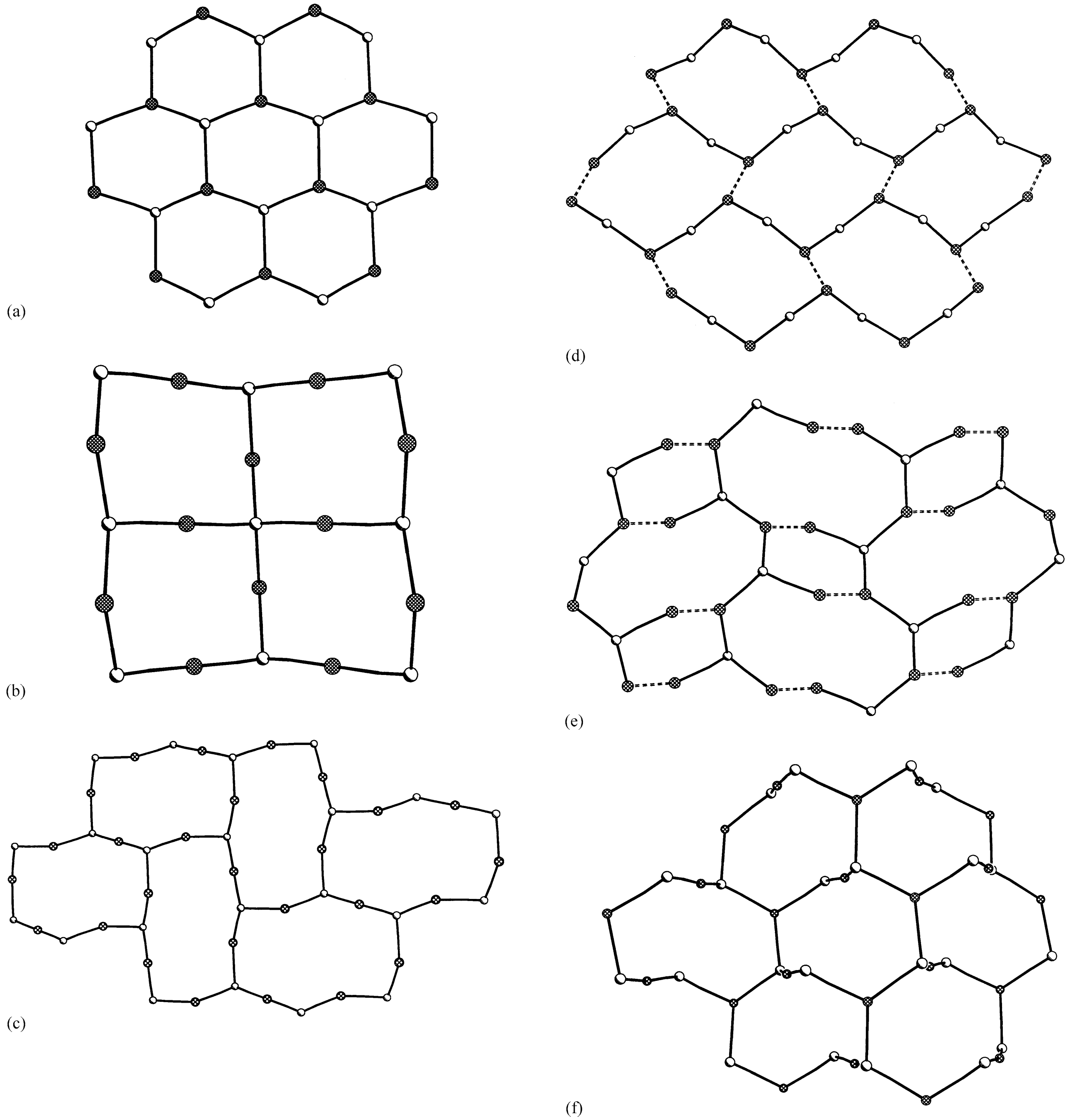

Fig. 5. Perspective views of topologic structural types of two-dimensional Ag–hmt nets for **13** (a), **22** (b), **26** (c), **27** (d), **28** (e) and **29** (f). Small open balls represent centers of mass of the hmt ligands, which were adapted from Ref. [20] for (a, b), Ref. [21] for (c) and Ref. [24] for (d–f).

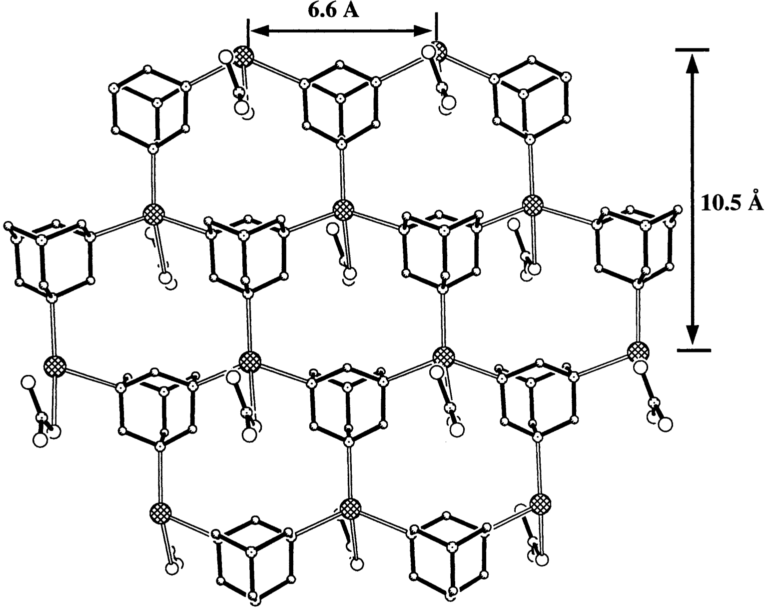

Fig. 6. The two-dimensional layer viewed along the *a*-axis direction in **13** (adapted from Ref. [12]).

ture type [17]. The structure consists of an infinite cationic array composed of almost planar hexagonal units of six hmt molecules linked by biconnected Ag(I) atoms, which are further interconnected by unique trigonal [Ag · N3] center into a three-dimensional networks with large cavities and channels of the hexagonal sections (Fig. 8), containing PF_6^- anions and solvent molecules as guests. As shown in Fig. 9, [Ag(μ_3-hmt)](PF_6) · H_2O (**31**) consists of an open three-dimensional cationic network with two types of channels [14]. The PF_6^- anions and guest water molecules occupy the large octagonal channels. In the topological point of view, the networks of **30** and **31** are all triconnected three-dimensional (3-D, 3-C) enantiomorphic interpenetrating networks.

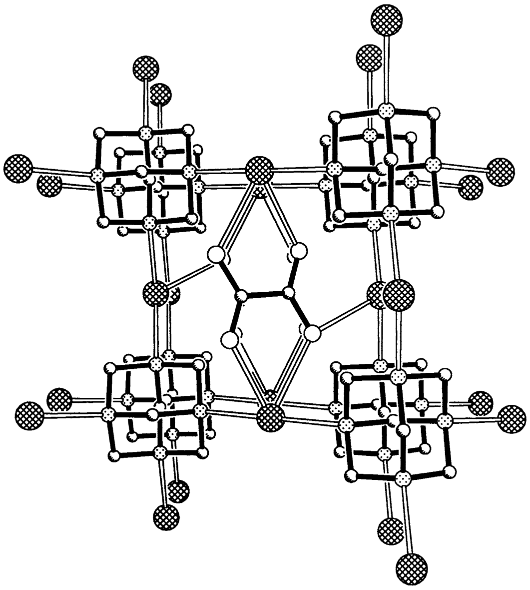

Fig. 7. The three-dimensional network viewed along the *b*-axis direction in **23** (adapted from Ref. [20]).

On the other hand, the Ag–hmt interactions in [Ag_{12}(μ_4-hmt)$_6$(HPO_4)(H_2PO_4)$_{10}$(H_2O)](H_3PO_4) · 10.5H_2O (**32**) furnish an open tetraconnected three-dimensional (3-D, 4-C) cationic network with three types of channels (Fig. 10) [20]. However, the HPO_4^{2-} and $H_2PO_4^-$ groups act in the μ_2-/μ_3-bridging and monodentate modes in coordination to the Ag(I) atoms, while the neutral H_3PO_4 molecule is hydrogen-bonded to the lattice water molecules and the coordinated HPO_4^{2-} or $H_2PO_4^-$ groups. As shown in Fig. 11 [Ag_2(μ_4-hmt)(NO_3)$_2$] (**33**) is another type of molecular-based framework with square units, topologically also related to the tetraconnected three-dimensional framework [15]. Each square unit consists of six Ag(I) atoms and six hmt ligands.

The structures of [Ag_3(μ_4-hmt)$_2$(H_2O)$_2$](ClO_4)$_3$ (**34**) and [Ag_3(μ_4-hmt)$_2$(H_2O)$_2$](SO_4)(HSO_4) · 2H_2O (**35**) consist of an open three-dimensional cationic network formed by [Ag(μ_3-hmt)] hexagonal layers joined by biconnected Ag(I) atoms, which coordinate to the fourth nitrogen atoms of the hmt ligands, as shown in Fig. 12 [16,20b]. The ClO_4^- and lattice water molecules in **34** or the SO_4^{2-}, HSO_4^- and lattice water molecules in **35** are clathrated in the hexagonal channels. Similarly, [Ag_3(μ_4-hmt)$_2$(μ_2-ssa)(H_2O)](NO_3) · 3H_2O (ssa = sulfosalicylate) (**36**) also consists of an open three-dimensional cationic network formed by [Ag(μ_3-hmt)] hexagonal layers joined by biconnected Ag(I) atoms, however, the locations of biconnected Ag(I) atoms are different, resulting in an interesting open three-dimensional cationic network with two types of channels, as shown in Fig. 13 [29]. The large hexagonal unit

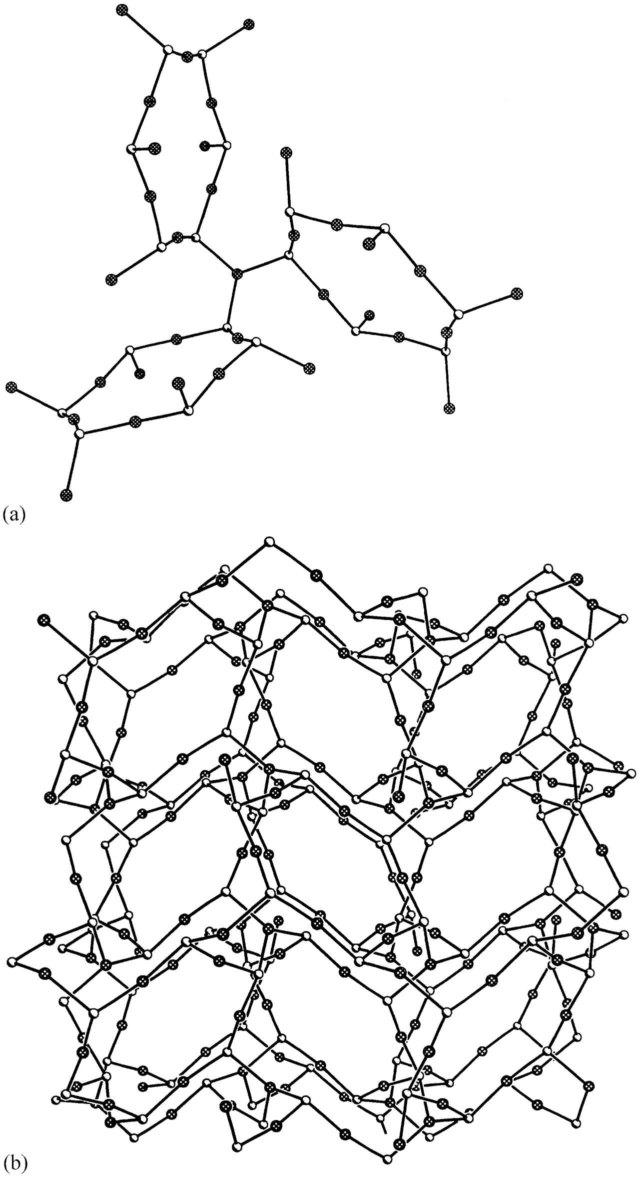

Fig. 8. Perspective views of the unique trigonal [Ag · N3] center (a) and the three-dimensional networks with large cavities projected along the *c*-axis in **30** (adapted from Ref. [17]). Small open balls represent centers of mass of the hmt ligands.

involves eight Ag(I) atoms and eight hmt ligands, while the small one involves four Ag(I) atoms and four hmt ligands. The ssa groups in large hexagonal channels interlink the adjacent undulating layers, while the nitrate counterions are clathrated in the small ones. In the structure of $[Ag_{11}(\mu_4\text{-hmt})_6(H_2O)_{10}](PF_6)_{11} \cdot 4H_2O$ (**37**) (Fig. 14), there are two types of parallel channels [18]. These channels host the PF_6^- anions and lattice water molecules. As shown in Fig. 15, $[Ag_4(\mu_4\text{-hmt})_3(H_2O)](SO_4)(NO_3)_2 \cdot 3H_2O$ (**38**) consists of an interesting open three-dimensional cationic network with two types of channels [20b]. The large hexagonal unit involves six Ag(I) atoms and six hmt ligands, while the small one involves four Ag(I) atoms and four hmt ligands. The SO_4^{2-} anions and lattice water molecules are clathrated in the large hexagonal unit, while the NO_3^- anions are clathrated in the small ones. This fact implies that the counter anions may play a role in templating the channel structure.

In $[Ag_2(\mu_4\text{-hmt})(\mu_2\text{-}O_2CMe)](MeCO_2) \cdot 4.5H_2O$ (**39**), the hexagonal sub-unit viewed from the *c*-axis direction involves four Ag(I) atoms, two dimeric Ag(I) fragments and six hmt ligands (Fig. 16) [20a]. It should be noted that the dimeric Ag(I) fragments are joined by two unusual non-coplanar skew–skew μ_2-carboxylate bridges with the Ag· · · Ag distance of 2.914(1) Å, showing significant Ag· · · Ag interaction [31]. The topology of the Ag–hmt interaction in $[Ag_2(\mu_4\text{-hmt})(\mu_3\text{-L})] \cdot nH_2O$ (L = maleate, diglycolate, *m*-phthalate) (**40**) is the same as that of **39** [20b,25].

As shown in Fig. 17, $[Ag_3(\mu_4\text{-hmt})(\mu_2\text{-ba})_3]$ (ba= benzoate) (**41**) is made up of a neutral three-dimensional honeycomb-like coordination network with hexagonal units [20b]. Each hexagonal unit viewed from the *a*-axis direction involves six dimeric Ag(I) fragments and six hmt ligands. As shown in Fig. 18, $[Ag_8(\mu_3\text{-hmt})_2(\mu_4\text{-hmt})_2(\mu_2\text{-pma})_2(\mu_2\text{-}H_2O)_3] \cdot 18H_2O$ (**42**) is another new type of three-dimensional non-interpenetrated network with cylindrical channels [29], in which there are two different types of hmt molecules acting in μ_3-bridging and μ_4-bridging modes, respectively. Moreover, the network is further stabilized by the bis-monodentate pma ligands and unprecedented μ_2-aquo-oxygen atoms. **39**–**42** are all constructed by dimeric Ag(I) fragments in the three-dimensional Ag–hmt networks. Moreover, **34**–**42** are all topologically related to the tri- and tetra-connected three-dimensional (3-D, 3,4-C) nets.

2.5. *Designed organization of three-dimensional microporous networks based on the hexagonal Ag–hmt layers*

Chemists hope to reach a stage at which rational designs and synthesis of interesting topologies, as well as molecular solids with potentially interesting properties are possible [2,34,35]. For practical uses of this kind of materials, designed or controlled assembly is critically important. In Ag–hmt system, some designed organization of layers into three-dimensional architectures bearing microporous have been reported so far.

As mentioned in Section 2.3, the stable two-dimensional undulating coordination layers $[Ag(\mu_3\text{-hmt})X]$ (X = small and labile anions) of hexagonal units in a boat-type conformation (see Fig. 5a and Fig. 6), which bear labile lateral monodentate ligands such as nitrate and perchlorate can easily be obtained. Careful examination of the detailed geometric data also reveals that the labile ligands (and the metal atoms) are arranged in rows with regular intra-row spacing of ca. 6.6 Å, which is about twice of the face-to-face distance between a pair of strongly stacked aromatic groups

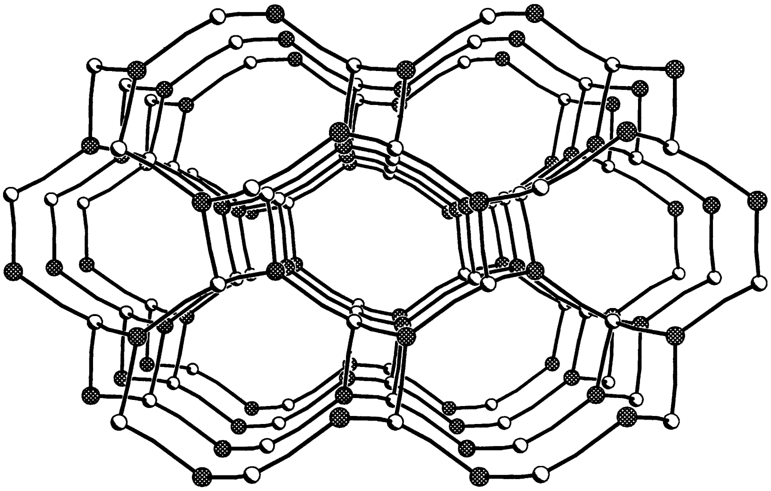

Fig. 9. The three-dimensional cationic network with two types of channels viewed along the *b*-axis in **31** (adapted from Ref. [14]). Small open balls represent centers of mass of the hmt ligands.

(Fig. 6) [12]. In fact, after **11–13** were obtained, two routes for rational organization of the two-dimensional hexagonal Ag–hmt coordination layers into some kinds of three-dimensional networks were established (Scheme 3) [23]. The first route is using aromatic monocarboxylates, having ability of π–π stacking interaction, to replace the small and labile ions of the two-dimensional [Ag(μ_3-hmt)X] (X = small and labile anions) layer, the resulting layers can be further extended into three-dimensional supramolecular arrays via intercalation between the lateral aromatic groups. The second route is using the bridging dicarboxylate spacers (or molecular pillars) to replace the small and labile ions of the [Ag(μ_3-hmt)X] layer, the adjacent two-dimensional layers can be, therefore, pillared into stable three-dimensional coordination networks with tunable channels. Complexes [Ag(μ_3-hmt)(L)] · nH$_2$O (L = 4-nitrobenzoate, 3-nitrobenzoate, 3,5-dinitrobenzoate) (**15**) (Fig. 19) and [Ag$_2$(μ_3-hmt)$_2$(L)] · nH$_2$O (L = fumarate, adipate, *p*-phthalate) (**16**) (Fig. 20), featuring small channels, were obtained by this rational design and synthesis, and the microporosity was confirmed by the gas adsorption measurements [23].

However, as shown in Scheme 4, there are different interconnection modes of the hexagonal units in the [Ag (μ_3-hmt)] layers and different bonding interactions between Ag(I) atoms and lateral ligands. In [Ag(μ_3-hmt)(L)] · nH$_2$O · mEtOH (L = 1-hydroxy-2-naphthate, 3-hydroxy-2-naphthate, 2-naphthoxyacetate) (**17**) [23] and [Ag(μ_3-hmt)(L)] · nH$_2$O (L = malonate, benzoate, salicylate) (**18**) [26], the bonding interactions between the Ag(I) atoms and the lateral ligands are somewhat weak, which may be responsible for the different interconnection modes of the hexagonal units, the different lateral ligands as well as the different slanted ori-

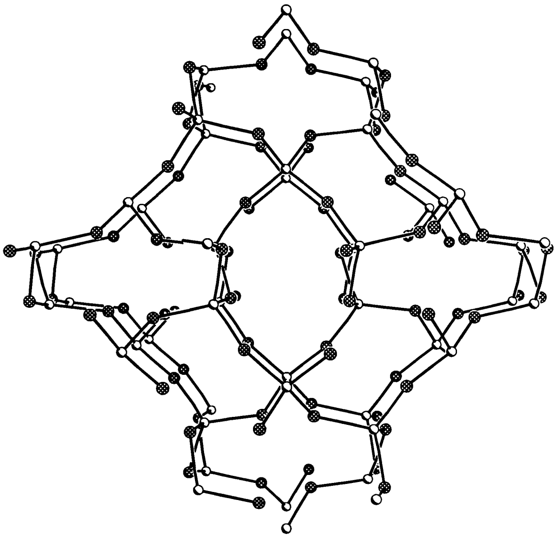

Fig. 10. The three-dimensional cationic network exhibiting three types of channels viewed along the *a*-axis in **32** (adapted from Ref. [20]). The H_3PO_4, $H_2PO_4^-$ and HPO_4^{2-} groups are omitted for clarity. Small open balls represent centers of mass of the hmt ligands.

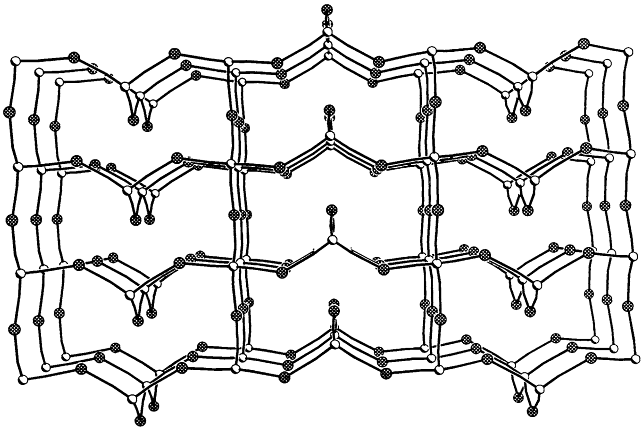

Fig. 11. The three-dimensional coordination network viewed along the *b*-axis in **33** (adapted from Ref. [15]). The NO_3^- bridges are omitted for clarity. Small open balls represent centers of mass of the hmt ligands.

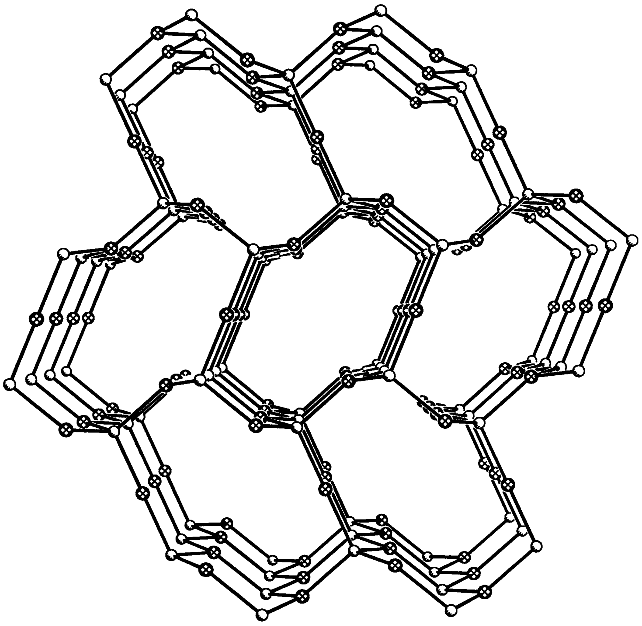

Fig. 12. The three-dimensional coordination network projected along the *c*-axis in **34** (adapted from Ref. [20]). Small open balls represent centers of mass of the hmt ligands.

entation modes of the lateral ligands, as shown in Fig. 21a, b and Scheme 4b, c. Moreover, the large naphthate groups in **17** may exclude their orientation in a similar mode found in **18** due to the mutual repulsion between the naphthate groups. On the other hand, the similar layer topology in **19** was observed (Fig. 21c and Scheme 4d), which may arise even though the lateral MeCN ligand is a stronger ligand because there are trigonally coordinated Ag(I) centers in the layer. Such three-coordinate centers alter the interconnection mode of the hexagonal units. The most significant structural feature presented here for **18** and **19** is that the two-dimensional [Ag(μ_3-hmt)] layers of hexagonal units in a boat-type conformation are highly undulated, and each pair of adjacent lateral ligands at the same side of the layers are slanted to each other, resulting in new two-dimensional coordination frameworks comprising micropores, as illustrated in Scheme 5.

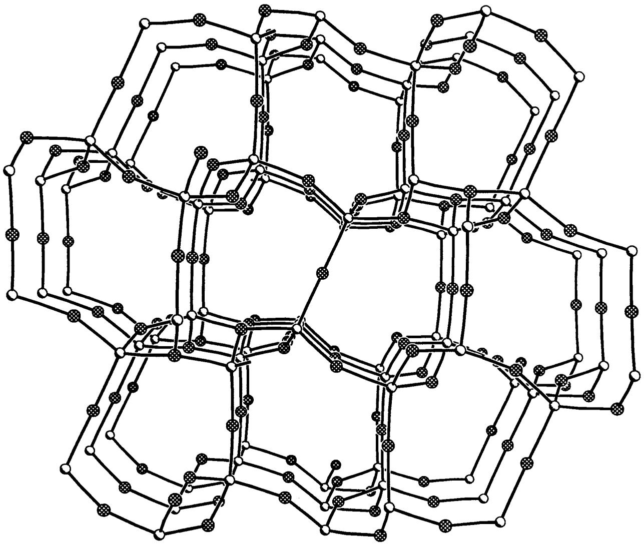

Fig. 14. The three-dimensional coordination network viewed along the *b*-axis in **37** (adapted from Ref. [18]). Small open balls represent centers of mass of the hmt ligands.

Furthermore, both the stability of the hexagonal two-dimensional layers [23,26] and weak coordination ability of sulfonate [36] may exclude any significant coordination interaction between the hexagonal two-dimensional layers and the sulfonate groups in [Ag(μ_3-hmt)](L) · *n*(benzene) · *m*H_2O (L = abs, ns) (**20**), where the contacts between the silver(I) and sulfonate oxygen atoms are all larger than 2.70 Å, well beyond those (2.38–2.62 Å) reported for other silver(I) sulfonate complexes [36], indicating only weak Ag· · ·O inter-

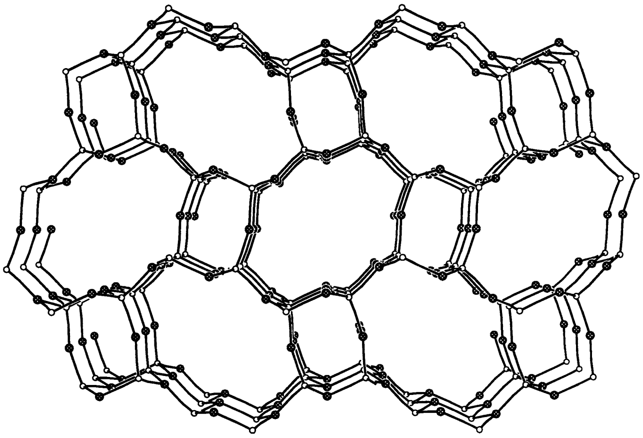

Fig. 13. The three-dimensional coordination network viewed along the *c*-axis in **36** (adapted from Ref. [29]). Small open balls represent centers of mass of the hmt ligands. The ssa groups bridges are omitted for clarity. Small open balls represent centers of mass of the hmt ligands.

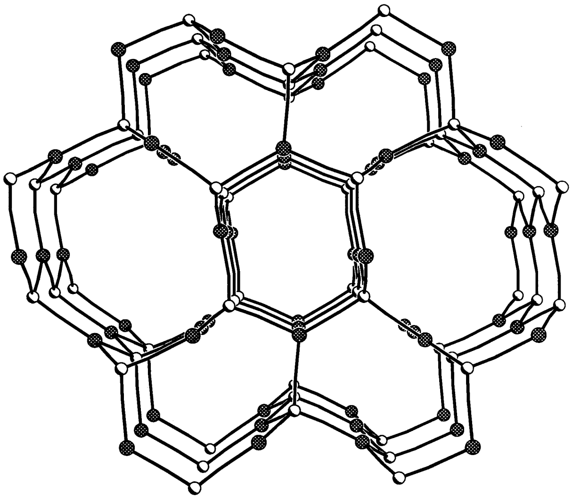

Fig. 15. The three-dimensional coordination network viewed along *b*-axis direction in **38** (adapted from Ref. [20]). Small open balls represent centers of mass of the hmt ligands.

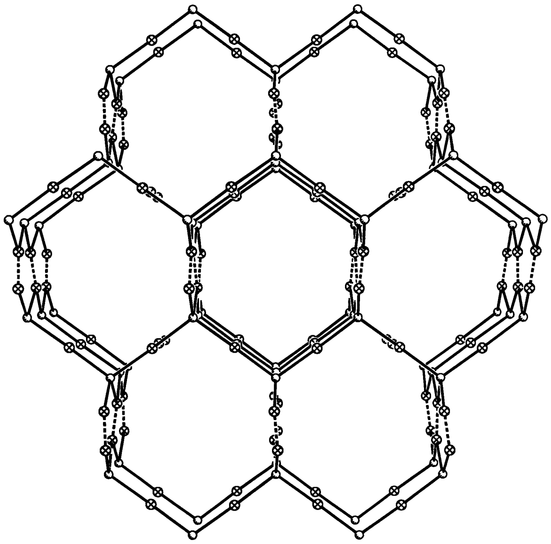

Fig. 16. The three-dimensional network of **39** viewed along the *c*-axis direction (adapted from Ref. [20]). The μ_2-O_2CMe bridges are omitted for clarity. Small open balls represent centers of mass of the hmt ligands.

actions, as shown in Fig. 22 [28]. Similar to the sulfonate, the pma ligands in $[Ag(\mu_3\text{-hmt})]_2[Ag(NH_3)_2]_2(pma) \cdot 3H_2O$ (**21**) connect with the Ag(I) atoms in the layers with the weak Ag···O contacts [28]. The isolation of these complexes shows that supramolecular interactions may be used in pillaring coordination layers into three-dimensional molecular architectures.

2.6. Ag–hmt coordination polymers exhibiting unique metal–π interactions

As discussed above, the combinations of hmt as a polydentate ligand and silver(I) can produce a wide variety of supramolecular architectures. By careful control of reaction conditions together with selection of appropriate ligands, a large number of open frameworks have been prepared. Meanwhile, synthetic approaches are also important. The liquid diffusion method has been employed in the preparation of silver(I) complexes of polycyclic aromatic compounds [37], and can be extended to obtain organosilver(I) complexes with aromatic carboxylate ligands based on Ag–hmt coordination networks with judicious choice of different aromatic carboxylate ligands.

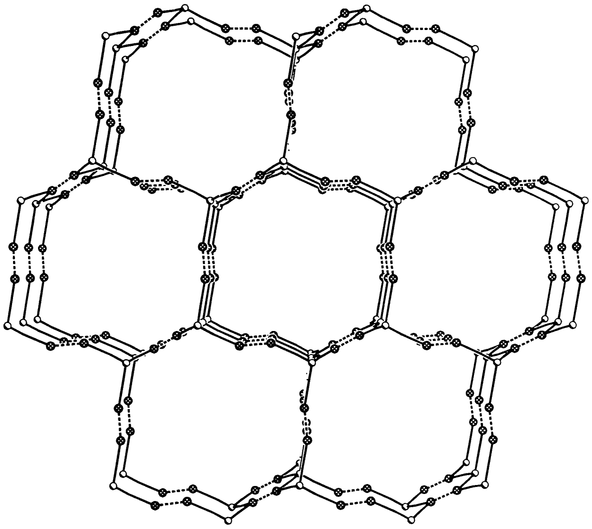

Fig. 17. The three-dimensional network of **41** viewed along the *a*-axis direction (adapted from Ref. [20]). The μ_2-ba bridges are omitted for clarity and small open balls represent centers of mass of the hmt ligands.

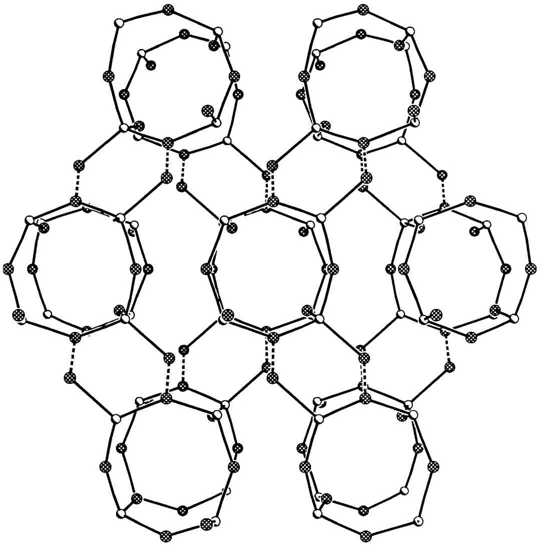

Fig. 18. Three-dimensional network of **42** viewed along the *c*-axis (adapted from Ref. [29]). The μ_2-pma bridges and lattice water molecules are omitted for clarity. Small open balls represent centers of mass of the hmt ligands.

$[Ag_4(\mu_4\text{-hmt})(\mu_4\text{-}\eta^2\text{-nda})_2] \cdot 2H_2O$ (**2**), $[Ag_2(\mu_2\text{-hmt})_2(\mu_2\text{-bi-}\eta^2\text{-bna})] \cdot 2H_2O \cdot MeCN$ (**5**) and $[Ag_2(\mu_4\text{-hmt})(\eta^2\text{-}\alpha\text{-hna})(MeCN)](\alpha\text{-hna}) \cdot H_2O$ (α-hna = 1-hydroxy-2-naphthate) (**25**) were obtained from the reaction of silver(I) aromatic carboxylates in MeCN solution with hmt in CH_2Cl_2 solution via the liquid diffusion method [27]. In these complexes, hmt exhibit different coordination modes, resulting in different Ag–hmt frameworks: the unique [hmt · 4Ag(I)] structural units in **2**, infinite zigzag $[Ag(\mu_2\text{-hmt})]_\infty$ chains in **5**, and two-dimensional infinite undulating cationic layers of square units in **25**. **2** is actually extended into a three-dimensional structure through the carboxylate bridges. The most significant structural feature presented here is the aromatic carboxylates ligated to the metal atoms via a unique η^2 coordination mode involving their aromatic rings, in addition to the normal coordination modes utilizing their carboxylate oxygen atoms. The Ag–C separations ranging from 2.433(6) to 2.710(9) Å in these complexes fall within the values reported for the silver(I) complexes of other polycyclic aromatic compounds [37], indicating significant Ag–C or Ag–π bonding interactions. For example, the nda ligand in **2** exhibits the unique μ_2-O-bridging-bidentate-η^2-coordination mode as shown in Fig. 23. All the complexes show interesting electrochem-

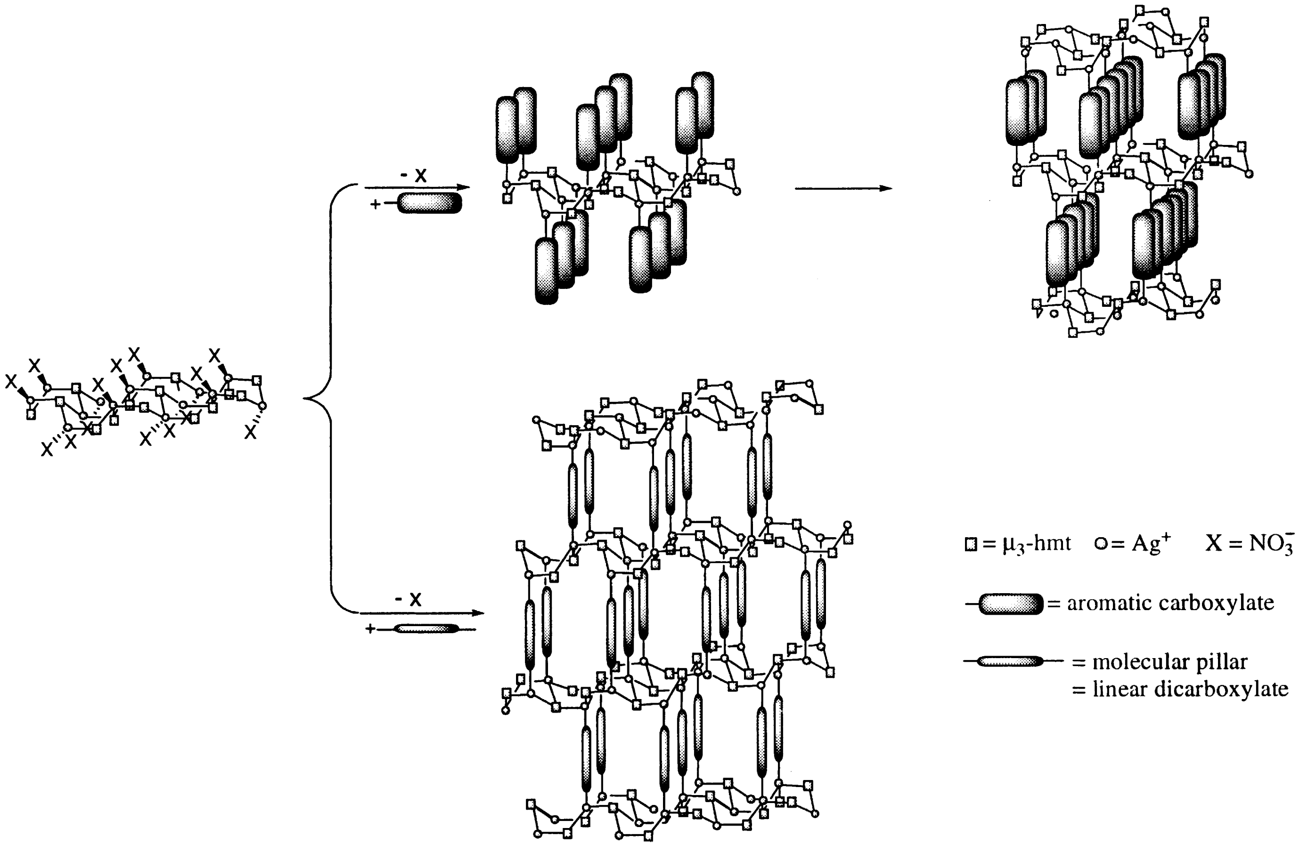

Scheme 3. Two routes for rational organization of the two-dimensional hexagonal Ag–hmt coordination layers into three-dimensional networks (adapted from Ref. [23]).

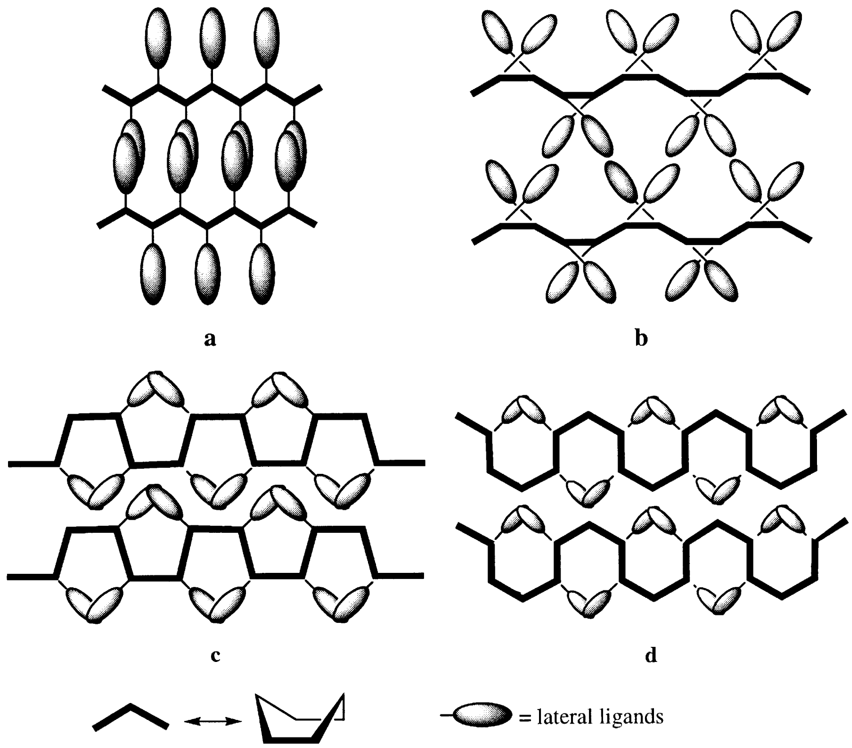

Scheme 4. Four interconnection modes of the hexagonal units in two-dimensional [Ag(μ_3-hmt)] layers in **15** (a), **17** (b), **18** (c), and **19** (d), which were adapted from Ref. [23] for (a, b) and Ref. [26] for (c, d).

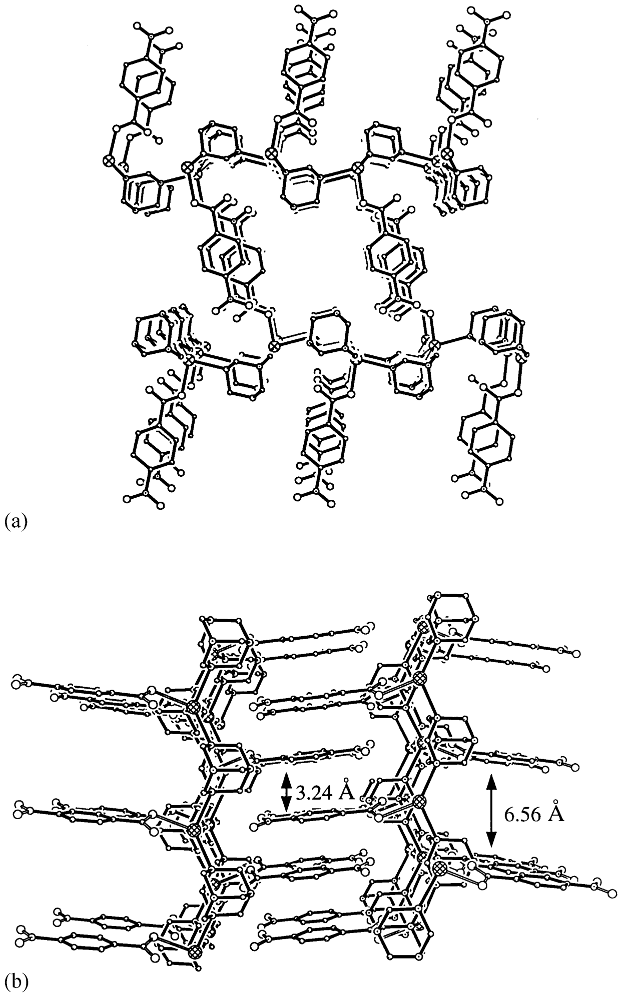

Fig. 19. The three-dimensional network of viewed along the *a*-axis (a) and *c*-axis (b) in **15** (adapted from Ref. [23]). The lattice water molecules are omitted for clarity.

ical and magnetic properties analogous to those of silver(I) complexes of polycyclic aromatic compounds reported previously. Both **2** and **5** exhibit strong blue photoluminescence at room temperature. A similar η^1 Ag–π bonding interaction [Ag–C 2.688(8) Å] was found in $[Ag_2(\mu_4\text{-hmt})(tos)]$ (**24**) (tos = *p*-toluenesulfonate), which was also obtained by the liquid diffusion method [21]. The carboxylate complexes exhibiting Ag–π bonding interactions are unique and have not been obtained by other preparation methods. Therefore, the liquid diffusion approach provides a new strategy for the preparation of air-stable multidimensional metal–organic coordination polymers with metal–aromatic interaction.

3. Synthetic chemistry

3.1. The important factors influencing the Ag–hmt nets

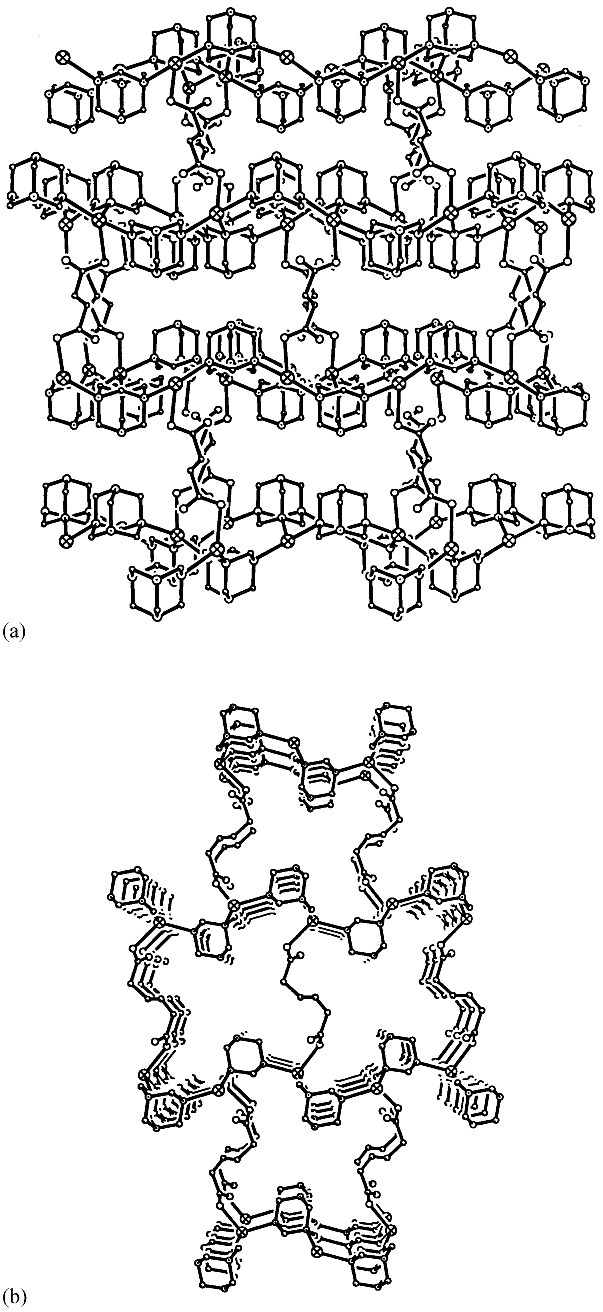

Fig. 20. The three-dimensional coordination networks of $[Ag_2(\mu_3\text{-hmt})_2(L)]\cdot 4H_2O$ (**16**) viewed along the *c*-axis: (a) for L = fa and (b) for L = adp, (adapted from Ref. [23]). The lattice water molecules are omitted for clarity.

The self-assembly of coordination frameworks is highly influenced by factors such as the solvent system, template, the pH value of the solution and steric requirement of the counterion [1,38]. Investigations on the Ag–hmt species further demonstrate that different frameworks can be obtained upon varying the counterions, molar ratio of metal-to-hmt, pH values of the solutions and/or solvent system.

For example, in the reactions of hmt with $AgPF_6$, different coordination polymers, $[Ag_5(\mu_2\text{-hmt})_6](PF_6)\cdot 3CH_2Cl_2$ (**3**) [17], $[Ag_3(\mu_3\text{-hmt})_2(H_2O)_4](PF_6)_3$ (**26**) [21], $[Ag_4(\mu_3\text{-hmt})_3(H_2O)](PF_6)_4\cdot 3EtOH$ (**30**) [17], $[Ag(\mu_3\text{-hmt})](PF_6)\cdot H_2O$ (**31**) [14] and $[Ag_{11}(\mu_4\text{-hmt})_6(H_2O)_{10}](PF_6)_{11}\cdot 4H_2O$

(**37**) [18], have been isolated, exhibiting Ag/hmt ratios in the range of 0.833:1–1.8:1, which illustrates the complicated nature of the reaction processes. In the reactions of hmt with $AgNO_2$, two different adducts, in which one contains two-dimensional hexagonal layers (Ag/hmt = 1:1 in $[Ag(\mu_3\text{-hmt})(NO_2)]$ (**13**) [20b]) and the other contains two-dimensional square layers (Ag/hmt = 2:1 in $[Ag_2(\mu_4\text{-hmt})(NO_2)]$ (**22**) [20b]), were obtained under different molar ratios of metal-to-hmt. Similarly, the isolation of different products could be achieved with $AgClO_4$ and $AgNO_3$. These two salts give 1:1 adducts, $[Ag(\mu_3\text{-hmt})](ClO_4)$ (**11**) [16] and $[Ag(\mu_3\text{-hmt})(NO_3)]$ (**13**) [12], that contain quite similar two-dimensional hexagonal layers; whereas in the presence of excessive silver(I) ions, three-dimensional frameworks with hmt ligands, all four-connected, are recovered in both cases, $[Ag_3(\mu_4\text{-hmt})_2(H_2O)_2](ClO_4)_3$ (**34**) [16] and $[Ag_2(\mu_4\text{-hmt})(NO_3)_2]$ (**33**) [15], but showing a different stoichiometry.

On the other hand, for the same ligands, different bonding interactions can also result in different coordination

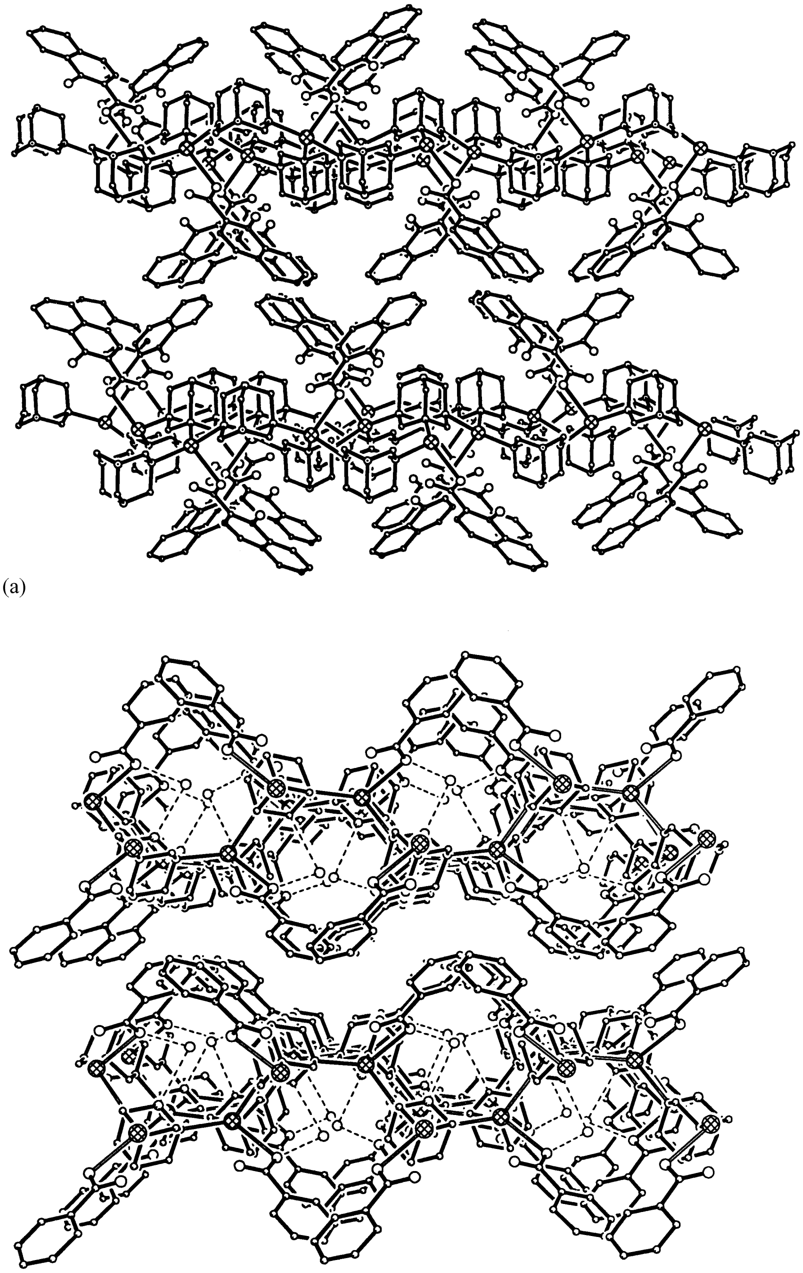

(a)

(b)

Fig. 21. The packing of the layers viewed along the *b*-axis in **17** (a), viewed along the *a*-axis in **18** (b) and viewed along the *b*-axis in **19** (c), which were adapted from Ref. [23] for (a) and Ref. [26] for (b, c).

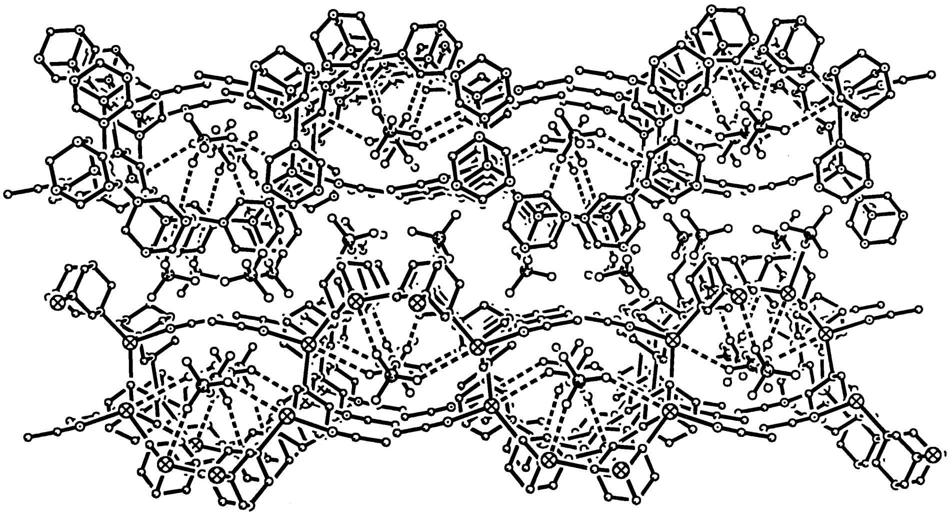

Fig. 21. (*Continued*).

frameworks under different pH values, such as the pair of complexes $[Ag_2(\mu_4\text{-hmt})(SO_4)(H_2O)]\cdot 4H_2O$ (**22**) and $[Ag_3(\mu_4\text{-hmt})_2(H_2O)_2](SO_4)(HSO_4)\cdot 2H_2O$ (**35**) [20] and the pair of complexes $[Ag(\mu_3\text{-hmt})]_2[Ag(NH_3)_2]_2(pma)\cdot 3H_2O$ (**21**) [28] and $[Ag_8(\mu_3\text{-hmt})_2(\mu_4\text{-hmt})_2(\mu_2\text{-pma})_2(\mu_2\text{-}H_2O)_3]\cdot 18H_2O$ (**42**) [29]. It should be noted that an Ag/hmt ratio of 1:1 does not ensure the formation of two-dimensional layered polymers, as shown by the one-dimensional ribbon structure of **4** [14] and the three-dimensional framework of **31** [14]. These observations may be attributed to the stronger influence of the counter anions than the equimolar Ag–hmt effect. Furthermore, the isolation of $[Ag_3(\mu_4\text{-hmt})_2(\mu_2\text{-ssa})(H_2O)](NO_3)\cdot 3H_2O$ (**36**) and $[Ag_4(\mu_4\text{-hmt})_3(H_2O)](SO_4)(NO_3)_2\cdot 3H_2O$ (**38**) indicates that the Ag–hmt complexes containing multiple types of counterions may exhibit different topological motifs compared with those containing a single type of counterions [29].

The three-dimensional Ag–hmt networks are usually obtained in the presence of either uncoordinated counterions or additional strongly bridging ligands in the reaction systems, whereas the two-dimensional networks are easily generated in the presence of monodentate ligands. Thus, the complexes may exhibit different, but related structures by judicious choice of different anionic ligands, such as **6–10** [22].

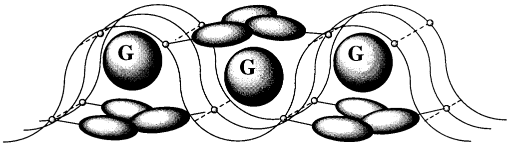

Scheme 5. Schematic representation of the topological motif of the two-dimensional microporous coordination layer based on a corrugated sheet (adapted from Ref. [26]).

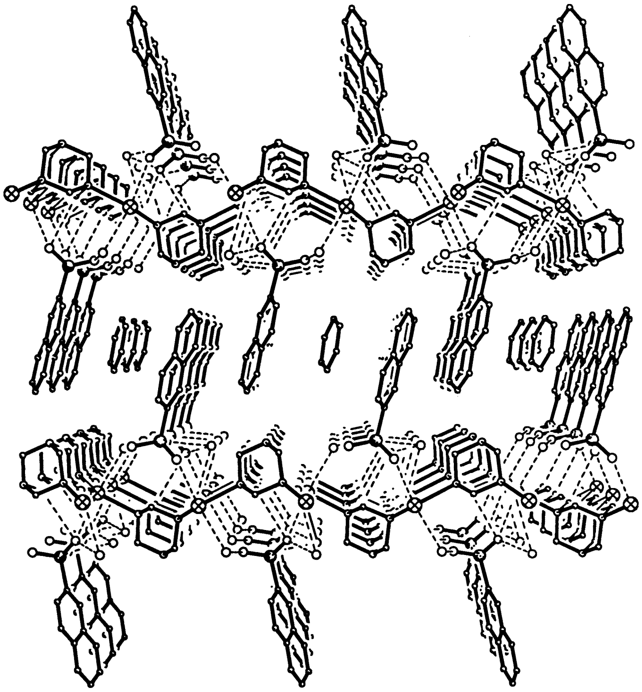

Fig. 22. Perspective view of the three-dimensional molecular architecture viewed along the *c*-axis in **20** (adapted from Ref. [28]). The C–H···O hydrogen bonds are omitted for clarity.

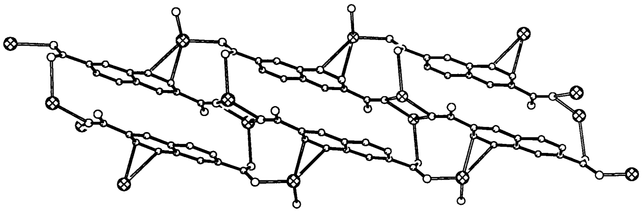

Fig. 23. The unique μ_2-O-bridging-bidentate-η^2-coordination mode of the 2,6-naphthalenedicarboxylate ligands in **2** (adapted from Ref. [27]).

Most of the Ag–hmt coordination polymers have been prepared in the conventional evaporation method. The several examples of Ag–hmt–aromatic carboxylate isolated by liquid diffusion method imply that the crystallization approach is also important. The Ag–π compounds were usually generated by the diffusion method.

3.2. Designed organization of two-dimensional nets into three-dimensional architectures

Supramolecular interactions such as π–π stacking interaction is important and can be used in the designed assembly of interesting microporous networks based on two- dimensional Ag–hmt coordination layers, as discussed in Section 2.5. Such rational assembly is based on two important factors, the geometric structure of the two-dimensional nets and the substitutability of the lateral ligand. Fortunately, the two-dimensional layer of $[Ag(\mu_3\text{-hmt})X]$ (X = small and labile anions) satisfy the requirements, although not all substituted aromatic ligands can be expected to furnish the aromatic intercalation for generation of the designed three-dimensional architecture!

The rational assembly of coordination layers via aromatic groups intercalation to generate three-dimensional architectures could also be utilized in the organization of low-dimensional coordination polymers and inorganic–organic hybrid materials into ordered three-dimensional architectures. Several examples have recently been reported [34,39]. Meanwhile, studies have shown that several linear dicarboxylate can be used to pillar the Ag–hmt coordination layers to produce the porous three-dimensional architectures with variable channels, mainly depending on the lengths of the carboxylate pillars.

In other words, an appropriate selection of the monocarboxylate and dicarboxylate can possibly result in the generation of designed three-dimensional structures with different channels.

4. Conclusions

This article summarizes recent progress on the construction of Ag(I)–hmt networks, including the interesting topologies, synthetic approaches and the important factors that influence the structures, as well as some designed assembly approaches. Remarkable progress in this field has been made in the last several years. A great significance has been demonstrated in the previous studies that, simple silver(I) ions and hmt ligand can be utilized in the construction of intriguing coordination polymeric architectures depending on Ag/hmt ratios, counterions, additional organic ligands, as well as other reaction and crystallization conditions. It may be expected that porous organometallic materials and interesting molecular architectures with new topologies can be achieved through controlled solid-state design using the Ag–hmt or other simple metal–ligand systems.

Acknowledgements

This work was supported by the National Natural Science Foundation of China (No. 20001008 and 29971033) and the Ministry of Education of China.

References

[1] (a) S.R. Batten, R. Robson, Angew. Chem. Int. Ed. 37 (1998) 1460;
(b) O.M. Yaghi, H. Li, C. Davis, D. Richardson, T.L. Groy, Acc. Chem. Res. 31 (1998) 474;
(c) A.J. Blake, N.R. Champness, P. Hubberstey, W.-S. Li, M.A. Withersby, M. Schröder, Coord. Chem. Rev. 183 (1999) 117;
(d) P.J. Hagrman, D. Hagrman, J. Zubieta, Angew. Chem. Int. Ed. 38 (1999) 2639;
(e) B. Moulton, M.J. Zaworotko, Chem. Rev. 101 (2001) 1629.

[2] (a) K.R. Seddon, M. Zaworotko, Crystal Engineering: the Design and Application of Functional Solids, Kluwer Academic Publishers, Dordrecht, 1999;
(b) D. Braga, F. Grepioni, A.G. Orpen, Crystal Engineering: from Molecules and Crystals to Materials, Kluwer Academic Publishers, Dordrecht, 1999;
(c) G.W. Gokel, Advances in Supramolecular Chemistry, Vol. 7, JAI Press, Greenwich, 2000.

[3] (a) Y.-C. Liang, R. Cao, W.-P. Su, M.-C. Hong, W.-J. Zhang, Angew. Chem. Int. Ed. 39 (2000) 3304;
(b) M.J. Zaworotko, Chem. Commun. 39 (2001) 1.

[4] (a) H. Li, M. Eddaoudi, M. O'Keeffe, O.M. Yaghi, Nature 402 (1999) 276;
(b) S.S.Y. Chui, S.M.F. Lo, J.P.H. Charmant, A.G. Orpen, I.D. Williams, Science 283 (1999) 1148;
(c) S.-I. Noro, S. Kitagawa, M. Kondo, K. Seki, Angew. Chem. Int. Ed. 39 (2000) 2081.

[5] (a) F.A. Mautner, R. Cortes, L. Lezama, T. Rojo, Angew. Chem. Int. Ed. Engl. 35 (1996) 78;
(b) K. Inoue, T. Hayamizu, H. Iwamura, D. Hashizume, Y. Ohashi, J. Am. Chem. Soc. 118 (1996) 1803;
(c) M.-L. Tong, X.-M. Chen, B.-H. Ye, L.-N. Ji, Angew. Chem. Int. Ed. 38 (1999) 2237.

[6] (a) B. Moulton, J.-J. Lu, M.J. Zaworotko, J. Am. Chem. Soc. 123 (2001) 9224;
(b) A.N. Khlobystov, A.J. Blake, N.R. Champness, D.A. Lemenovskii, A.G. Majouga, N.V. Zyk, M. Schröder, Coord. Chem. Rev. 222 (2001) 155.

[7] (a) G.R. Dickinson, A.L. Raymond, J. Am. Chem. Soc. 45 (1923) 22;
(b) R.G.W. Wyckoff, R.B. Corey, Z. Kristallogr. 89 (1934) 462.

[8] T.C.W. Mak, G.-D. Zhou, Crystallography in Modern Chemistry, Wiley, New York, 1992 and references therein.

[9] (a) V.B. Gaillard, W. Paciorek, K. Schenk, G. Chapuis, Acta Crystallogr. Sect. B 52 (1996) 1036;
(b) D. Schwarzenbach, M. Bonin, Acta Crystallogr. Sect. B 55 (1999) 448;
(c) A.J. Lough, P.S. Wheatley, G. Ferguson, C. Glidewell, Acta Crystallogr. Sect. B 56 (2000) 261;
(d) W. Li, J.-P. Zhang, M.-L. Tong, X.-M. Chen, Aust. J. Chem. 54 (2001) 213.

[10] K.Y. Hui, P.C. Chan, T.C.W. Mak, Inorg. Chim. Acta 84 (1984) 25.

[11] (a) I.A. Baidina, B.I. Imanakunov, T.A. Toktomatov, P.A. Stabnikov, Z. Neorg. Khim. 36 (1991) 775;
(b) R. Fuchs, P. Klufers, J. Organomet. Chem. 424 (1992) 353;
(c) J.B. Hill, S.J. Eng, W.T. Pennington, G.H. Robinson, J. Organomet. Chem. 445 (1993) 11;
(d) B. Stibr, J. Holub, T. Jelinek, X.L.R. Fontaine, J. Fusek, J.D. Kennedy, M. Thornton-Pett, J. Chem. Soc. Dalton Trans. 445 (1996) 1741;

(e) J. Pickardt, G.T. Gong, D. Roleke, Z. Naturforsch. Teil. B 49 (1994) 321;
(f) S.R. Batten, B.F. Hoskins, R. Robson, Chem. Eur. J. 6 (2000) 156;
(g) M.-L. Tong, S.-L. Zheng, X.-M. Chen, Acta Crystallogr. Sect. C 56 (2000) 960.

[12] A. Michelet, B. Voissat, P. Khodadad, N. Rodier, Acta Crystallogr. Sect. B 37 (1981) 2171.

[13] (a) T.C.W. Mak, Inorg. Chim. Acta 84 (1984) 19;
(b) T.C.W. Mak, Jiegou Huaxue (Chin. J. Struct. Chem.) 4 (1985) 16.

[14] L. Carlucci, G. Ciani, D.M. Proserpio, A. Sironi, J. Am. Chem. Soc. 117 (1995) 12861.

[15] O.M. Yaghi, H. Li, M. O'Keeffe, Mater. Res. Soc. Symp. Proc. 453 (1997) 127.

[16] L. Carlucci, G. Ciani, W.V. Gudenberg, D.M. Proserpio, A. Sironi, J. Chem. Soc. Chem. Commun. 453 (1997) 631.

[17] L. Carlucci, G. Ciani, D.M. Proserpio, A. Sironi, Inorg. Chem. 36 (1997) 1736.

[18] M. Bertelli, L. Carlucci, G. Ciani, D.M. Proserpio, A. Sironi, J. Mater. Chem. 7 (1997) 1271.

[19] (a)M.-L. Tong, S.-L. Zheng, X.-M. Chen, Proceedings of Second China–Korea Joint Symposium on Inorganic Chemistry, Nanjing, October 1998, pp. 29–3;
(b) W.M. Bu, L. Ye, Y.G. Fan, Inorg. Chem. Commun. 3 (2000) 194.

[20] (a) M.-L. Tong, S.-L. Zheng, X.-M. Chen, Chem. Commun. 3 (1999) 561;
(b) M.-L. Tong, S.-L. Zheng, X.-M. Chen, Chem. Eur. J. 6 (2000) 3729.

[21] L. Carlucci, G. Ciani, D.M. Proserpio, S. Rizzato, J. Solid State Chem. 152 (2000) 211.

[22] S.-L. Zheng, M.-L. Tong, X.-L. Yu, X.-M. Chen, J. Chem. Soc. Dalton Trans. 152 (2001) 586.

[23] S.-L. Zheng, M.-L. Tong, R.-W. Fu, X.-M. Chen, S.W. Ng, Inorg. Chem. 40 (2001) 3562.

[24] S.-L. Zheng, M.-L. Tong, H.-L. Zhu, Y. Fang, X.-M. Chen, J. Chem. Soc. Dalton Trans. 40 (2001) 2049.

[25] S.-L. Zheng, M.-L. Tong, Y. Fang, X.-M. Chen, Acta Chim. Sin. (Chin. Ed.) 59 (2001) 1442.

[26] S.-L. Zheng, M.-L. Tong, H.-L. Zhu, X.-M. Chen, New J. Chem. 59 (2001) 1425.

[27] S.-L. Zheng, M.-L. Tong, S.-D. Tan, Y. Wang, J.-X. Shi, Y.-X. Tong, H.K. Lee, X.-M. Chen, Organometallics 20 (2001) 5319.

[28] S.-L. Zheng, M.-L. Tong, X.-M. Chen, S.W. Ng, J. Chem. Soc. Dalton Trans. 20 (2002) 360.

[29] S.-L. Zheng, J.-P. Zhang, X.-M. Chen, S.W. Ng, J. Solid State Chem. 117 (2003) 45.

[30] (a) O. Ermer, J. Am. Chem. Soc. 110 (1988) 3747;
(b) G.R. Desiraju, Angew. Chem. Int. Ed. Engl. 34 (1995) 2311.

[31] S.-L. Zheng, M.-L. Tong, X.-M. Chen, Chin. J. Inorg. Chem. 18 (2002) 17.

[32] M. Jansen, Angew. Chem. Int. Ed. Engl. 26 (1987) 1098.

[33] (a) A.F. Wells, Three-Dimensional Nets and Polyhedra, Wiley, New York, 1977;
(b) I. Ino, L.-P. Wu, M. Munakata, M. Maekawa, Y. Suenaga, T. Kuroda-Sowa, Y. Kitamori, Inorg. Chem. 39 (2000) 2146;
(c) D.-L. Long, A.J. Blake, N.R. Champness, M. Schröder, Chem. Commun. 39 (2000) 1369;
(d) S.A. Barnett, A.J. Blake, N.R. Champness, J.E.B. Nicolson, C. Wilson, J. Chem. Soc. Dalton Trans. 39 (2001) 567;
(e) D.-L. Long, A.J. Blake, N.R. Champness, C. Wilson, M. Schröder, Chem. Eur. J. 8 (2002) 2026;
(f) D.J. Nielsen, A.M. Magill, B.F. Yates, K.J. Cavell, B.W. Skelton, A.H. White, Chem. Commun. 8 (2002) 2520.

[34] (a) H. Li, M. Eddaoudi, T.L. Groy, O.M. Yaghi, J. Am. Chem. Soc. 120 (1998) 8571;
(b) C.J. Kepert, M.J. Rosseinsky, Chem. Commun. 120 (1999) 375;
(c) Y.-H. Kiang, G.B. Gardner, S. Lee, Z. Xu, E.B. Lobkovsky, J. Am. Chem. Soc. 121 (1999) 8204;
(d) R.-G. Xiong, X.-Z. You, B.F. Abrahams, Z. Xue, C.-M. Che, Angew. Chem. Int. Ed. 40 (2001) 4422.

[35] (a) T.J. Prior, M.J. Rosseinsky, Chem. Commun. 5 (2001) 495;
(b) O.R. Evans, W. Lin, Acc. Chem. Res. 35 (2002) 511;
(c) M.D. Hollingsworth, Science 295 (2002) 2410.

[36] (a) G.K.H. Shimizeu, G.D. Enright, G.S. Rego, J.A. Ripmeester, Can. J. Chem. 77 (1999) 313;
(b) G.K.H. Shimizeu, G.D. Enright, C.I. Ratcliffe, K.F. Preston, J.L. Reid, J.A. Ripmeester, Chem. Commun. 77 (1999) 1485;
(c) G. Smith, B.A. Cloutt, D.E. Lynch, K.A. Byriel, C.H.L. Kennard, Inorg. Chem. 37 (1998) 3236;
(d) G. Smith, J.H. Thomasson, J.M. White, Aust. J. Chem. 52 (1999) 317.

[37] (a) M. Munakata, L.P. Wu, G.L. Ning, Coord. Chem. Rev. 198 (2000) 171;
(b) J.C. Zhong, M. Munakata, T. Kuroda-Sowa, M. Maekawa, Y. Suenaga, H. Konaka, Inorg. Chem. 40 (2001) 3191.

[38] (a) M.-L. Tong, B.-H. Ye, X.-M. Chen, S.W. Ng, Inorg. Chem. 37 (1998) 2645;
(b) L. Carlucci, G. Ciani, D.M. Proserpio, A. Sironi, Angew. Chem. Int. Ed. Engl. 34 (1995) 1895.

[39] (a) X.-M. Zhang, M.-L. Tong, S.-H. Feng, X.-M. Chen, J. Chem. Soc. Dalton Trans. 34 (2001) 2069;
(b) M.-L. Tong, Y.-M. Wu, S.-L. Zheng, X.-M. Chen, T. Yuen, C.L. Lin, X.-Y. Huang, J. Li, New J. Chem. 25 (2001) 1482;
(c) S. Lopez, S.W. Keller, Inorg. Chem. 38 (1999) 1883;
(d) C. Janiak, J. Chem. Soc. Dalton Trans. 38 (2000) 3885;
(e) S.-I. Noro, R. Kitaura, M. Kondo, S. Kitagawa, T. Ishii, H. Matsuzaka, M. Yamashita, J. Am. Chem. Soc. 124 (2002) 2568.